



A standardized pathology report for gastric cancer: 2nd edition

Young Soo Park^{1*}, Myeong-Cherl Kook^{2*}, Baek-hui Kim^{3*}, Hye Seung Lee^{4*}, Dong-Wook Kang⁵, Mi-Jin Gu⁶,
 Ok Ran Shin⁷, Younghee Choi⁸, Wonae Lee⁹, Hyunki Kim¹⁰, In Hye Song¹, Kyoung-Mee Kim¹¹, Hee Sung Kim¹²,
 Guhyun Kang¹³, Do Youn Park¹⁴, So-Young Jin¹⁵, Joon Mee Kim¹⁶, Yoon Jung Choi¹⁷, Hee Kyung Chang¹⁸,
 Soomin Ahn¹¹, Mee Soo Chang¹⁹, Song-Hee Han²⁰, Yoonjin Kwak⁴, An Na Seo²¹, Sung Hak Lee²², Mee-Yon Cho²³,

The Gastrointestinal Pathology Study Group of the Korean Society of Pathologists

¹Department of Pathology, Asan Medical Center, University of Ulsan College of Medicine, Seoul; ²Center for Gastric Cancer, National Cancer Center, Goyang;

³Department of Pathology, Korea University Guro Hospital, Seoul;

⁴Department of Pathology, Seoul National University Hospital, Seoul National University College of Medicine, Seoul;

⁵Department of Pathology, Chungnam National University Sejong Hospital, Chungnam National University School of Medicine, Sejong;

⁶Department of Pathology, Yeungnam University College of Medicine, Daegu;

⁷Department of Hospital Pathology, Uijeongbu St. Mary's Hospital, College of Medicine, The Catholic University of Korea, Uijeongbu;

⁸Department of Pathology, Hallym University Dongtan Sacred Heart Hospital, Hwaseong; ⁹Department of Pathology, Dankook University College of Medicine, Cheonan;

¹⁰Department of Pathology, Yonsei University College of Medicine, Seoul;

¹¹Department of Pathology and Translational Genomics, Samsung Medical Center, Sungkyunkwan University School of Medicine, Seoul;

¹²Department of Pathology, Chung-Ang University Hospital, Chung-Ang University College of Medicine, Seoul;

¹³LabGenomics Clinical Laboratories, Seongnam; ¹⁴St. Maria Pathology Laboratory, Busan; ¹⁵Department of Pathology, Soonchunhyang University Seoul Hospital, Seoul;

¹⁶Department of Pathology, Inha University School of Medicine, Incheon;

¹⁷Department of Pathology, Yongin Severance Hospital, Yonsei University College of Medicine, Yongin;

¹⁸Department of Pathology, Kosin University Gospel Hospital, Kosin University College of Medicine, Busan;

¹⁹Department of Pathology, Seoul National University Boramae Hospital, Seoul National University College of Medicine, Seoul;

²⁰Department of Pathology, Dong-A University College of Medicine, Busan;

²¹Department of Pathology, School of Medicine, Kyungpook National University, Kyungpook National University Chilgok Hospital, Daegu;

²²Department of Hospital Pathology, Seoul St. Mary's Hospital, College of Medicine, The Catholic University of Korea, Seoul;

²³Department of Pathology, Wonju Severance Christian Hospital, Yonsei University Wonju College of Medicine, Wonju, Korea

The first edition of 'A Standardized Pathology Report for Gastric Cancer' was initiated by the Gastrointestinal Pathology Study Group of the Korean Society of Pathologists and published 17 years ago. Since then, significant advances have been made in the pathologic diagnosis, molecular genetics, and management of gastric cancer (GC). To reflect those changes, a committee for publishing a second edition of the report was formed within the Gastrointestinal Pathology Study Group of the Korean Society of Pathologists. This second edition consists of two parts: standard data elements and conditional data elements. The *standard data elements* contain the basic pathologic findings and items necessary to predict the prognosis of GC patients, and they are adequate for routine surgical pathology service. Other diagnostic and prognostic factors relevant to adjuvant therapy, including molecular biomarkers, are classified as *conditional data elements* to allow each pathologist to selectively choose items appropriate to the environment in their institution. We trust that the standardized pathology report will be helpful for GC diagnosis and facilitate large-scale multidisciplinary collaborative studies.

Key Words: Stomach neoplasms; Gastrectomy; Endoscopic resection; Molecular pathology; Pathology report; Standardization

Received: December 1, 2022 **Revised:** December 22, 2022 **Accepted:** December 23, 2022

Corresponding Author: Sung Hak Lee, MD, PhD, Department of Hospital Pathology, Seoul St. Mary's Hospital, College of Medicine, The Catholic University of Korea, 222 Banpo-daero, Seocho-gu, Seoul 06591, Korea

Tel: +82-2-2258-1617, Fax: +82-2-2258-1627, E-mail: hakjang@catholic.ac.kr

Corresponding Author: Mee-Yon Cho, MD, PhD, Department of Pathology, Wonju Severance Christian Hospital, Yonsei University Wonju College of Medicine, 20 Ilson-ro, Wonju 26426, Korea

Tel: +82-33-741-1553, Fax: +82-33-731-6590, E-mail: meeyon@yonsei.ac.kr

*Young Soo Park, Myeong-Cherl Kook, Baek-hui Kim, and Hye Seung Lee contributed equally to this work.

This article has been published jointly, with consent, in both *Journal of Pathology and Translational Medicine* and *Journal of Gastric Cancer*.

Gastric cancer (GC) is the fifth most commonly diagnosed cancer and has the fourth-highest mortality rate worldwide [1]. Although the incidence and mortality rates of GC have decreased markedly during the past 50 years, Korean cancer registry data show that GC was still the most diagnosed cancer in 2018 [2]. The Gastrointestinal Pathology Study Group (GIPSG) of the Korean Society of Pathologists developed the first edition of 'A Standardized Pathology Report for Gastric Cancer' in 2005 to give pathologists a standard reporting format for GC diagnosis in daily practice [3].

Considerable changes in the pathology of GC have happened since then, such as the development of the histopathological classification for carcinoma and several pathologic features for prognostication [4,5]. In addition, molecular pathology tests for GC have become essential as treatment strategies for GC have developed rapidly, including advances in targeted therapy and immunotherapy [6,7]. Therefore, it is necessary to provide a second edition of the standardization report that reflects those changes.

In March 2022, a committee for revision of the report was formed within the GIPSG of the Korean Society of Pathologists. The committee consisted of subcommittees to discuss four topics: (1) radical resection specimens, (2) endoscopic resection specimens, (3) histologic classification, and (4) molecular markers for GC. This second edition of 'A Standardized Pathology Report for Gastric Cancer' was developed after several meetings of the subcommittees and entire committee.

The purpose of this report form is to standardize pathologic diagnosis of GC and enhance treatment capacity by facilitating communication between clinicians and pathologists. The basic pathologic findings for prognostication of GC are described in the "Standard data elements" section of the form, and other factors related to diagnosis and adjuvant therapy, including molecular biomarkers, are documented in the "Conditional data elements" section. A Korean version as well as an English version is also provided to enable Korean pathologists to use this report (Supplementary Material S1).

APPLICATION OF STANDARD PATHOLOGY REPORT

This standard pathology report is for use with primary gastric carcinomas. Neuroendocrine tumors, lymphomas, gastrointestinal stromal tumors, and other sarcomas are excluded. Carcinomas involving the esophagogastric junction (EGJ) with a center ≤ 2 cm into the proximal stomach are considered to be distal esophageal carcinoma and excluded, as defined in the American Joint

Committee on Cancer (AJCC), 8th edition [8]. This pathology report is also used for residual (post-chemotherapy or post-endoscopic resection) carcinomas. The report forms for pathologic diagnosis from radical resection and endoscopic resection specimens are shown in Tables 1 and 2, respectively.

Radical resection specimens

Gastrectomy (specimen) type

The type of surgical procedure should be mentioned in the surgical record.

Gross type

The gross type of each lesion should be recorded individually. The classification of early gastric cancer (EGC) uses the Japanese guideline (subclassification of type 0) [9], and classification of advanced gastric cancer (AGC) uses the Borrmann classification. The unclassifiable type is Borrmann type 5, according to the Japanese guideline [9]. The gross type is determined by macroscopic examination. If there is discrepancy between the macroscopic and microscopic findings, i.e., EGC on macroscopic examination but tumor invades the proper muscle microscopically (AGC), the macroscopic type should remain as the gross finding and not be corrected according to the microscopic finding. In such cases, the following descriptions are recommended: AGC, mimicking EGC type X or EGC, mimicking Borrmann type X. If the lesion is AGC grossly, at least four representative sections should be submitted for microscopic examination, including the deepest invasion, and ink should be applied at the serosal surface nearest the tumor. If the lesion is EGC grossly, grid mapping should be performed at 4 to 5 mm width.

Previous treatment

Any treatment before surgical resection should be recorded when applicable. If there are residual tumor foci, it should be mentioned that these are residual tumors. In post-chemotherapy gastrectomy situations, representative sections are sufficient if the lesion is large and obvious. However, the entire tumor bed must be microscopically examined when the representative sections contain no residual cancer cells or the residual lesion is small or inconspicuous grossly. For post-endoscopic resection specimens, the entire tumor bed should be submitted for microscopic evaluation.

Tumor focality

Tumor focality should record whether it is a single lesion or

Table 1. Report form for pathologic diagnosis using radical resection specimens

Standard and Conditional data elements
Gastrectomy (specimen) type^a <ul style="list-style-type: none"> <input type="checkbox"/> Total gastrectomy <input type="checkbox"/> Distal (subtotal) gastrectomy <input type="checkbox"/> Proximal gastrectomy <input type="checkbox"/> Wedge resection <input type="checkbox"/> Others (_____)
Gross type^a <ul style="list-style-type: none"> <input type="checkbox"/> EGC type <ul style="list-style-type: none"> <input type="checkbox"/> EGC type I/IIa/IIb/IIc/III <input type="checkbox"/> Mixed EGC type (_____) <input type="checkbox"/> AGC type <ul style="list-style-type: none"> <input type="checkbox"/> Borrmann type 1/2/3/4/unclassifiable <input type="checkbox"/> Others (_____)
Residual with previous treatment^a (when applicable) <ul style="list-style-type: none"> <input type="checkbox"/> Residual <input type="checkbox"/> Previous treatment <ul style="list-style-type: none"> <input type="checkbox"/> Chemotherapy <input type="checkbox"/> Chemoradiotherapy <input type="checkbox"/> Endoscopic mucosal resection <input type="checkbox"/> Endoscopic submucosal dissection <input type="checkbox"/> Unknown <input type="checkbox"/> Others (_____)
Tumor focality^a <ul style="list-style-type: none"> <input type="checkbox"/> Single <input type="checkbox"/> Multiple
Tumor location^a <ul style="list-style-type: none"> <input type="checkbox"/> Involvement <ul style="list-style-type: none"> <input type="checkbox"/> Esophagus/Upper/Middle/Lower third of the stomach/Duodenum <input type="checkbox"/> Center <ul style="list-style-type: none"> <input type="checkbox"/> Cardia/Fundus/Body/Antrum/Pylorus <input type="checkbox"/> Lesser curvature/Greater curvature/Anterior wall/Posterior wall <input type="checkbox"/> Others (_____)
Tumor size^a <p>One largest dimension</p> <input type="checkbox"/> ____ cm <p>Tumor size^b</p> <p>Secondary or tertiary tumor dimensions</p> <input type="checkbox"/> ____ × ____ cm <input type="checkbox"/> ____ × ____ × ____ cm
Histologic type^a <p>According to the principles described in "Histologic classification" section</p> <ul style="list-style-type: none"> <input type="checkbox"/> WHO <input type="checkbox"/> Lauren
Tumor regression grade^a (when applicable) <ul style="list-style-type: none"> <input type="checkbox"/> Grade 0: Complete response (no viable cancer cells) <input type="checkbox"/> Grade 1: Near complete response (single cells or rare small groups of cancer cells) <input type="checkbox"/> Grade 2: Partial response (residual cancer with evident tumor regression, but more than single cells or rare small groups of cancer cells) <input type="checkbox"/> Grade 3: Poor or no response (extensive residual cancer with no evident tumor regression)
Lymph node tumor regression^b (when applicable) <ul style="list-style-type: none"> <input type="checkbox"/> Not identified <input type="checkbox"/> Present
Depth of invasion (pT)^a <ul style="list-style-type: none"> <input type="checkbox"/> Invades lamina propria (pT1a) <input type="checkbox"/> Invades muscularis mucosae (pT1a) <input type="checkbox"/> Invades submucosa (sm1/sm2/sm3) (pT1b) <input type="checkbox"/> Invades proper muscle (pT2) <input type="checkbox"/> Invades subserosa (pT3) <input type="checkbox"/> Invades serosa (visceral peritoneum) (pT4a) <input type="checkbox"/> Directly invades adjacent structure (pT4b) specify (_____)
Resection margin^a <ul style="list-style-type: none"> <input type="checkbox"/> Proximal margin <ul style="list-style-type: none"> <input type="checkbox"/> Free from carcinoma (safety margin, ____ cm) <input type="checkbox"/> Involved by carcinoma

(Continued to the next page)

Table 1. Continued

Standard and Conditional data elements
<input type="checkbox"/> Distal margin <input type="checkbox"/> Free from carcinoma (safety margin, ___ cm) <input type="checkbox"/> Involved by carcinoma
Circumferential resection margin^b <i>Applied in EGJ or cardia cancer</i> <input type="checkbox"/> Free from carcinoma (safety margin, ___ cm) <input type="checkbox"/> Involved by carcinoma
Regional lymph node metastasis^a <i>At least 16 regional lymph nodes should be assessed</i> <input type="checkbox"/> no metastasis in ___ regional lymph nodes <input type="checkbox"/> metastasis in ___ out of ___ regional lymph nodes
Extranodal tumor extension^b <input type="checkbox"/> Not identified <input type="checkbox"/> Present
Isolated tumor cell clusters^b <i>Applied in incidentally identified tumor cell cluster less than 0.2 mm in greatest dimension with no other regional lymph node metastasis (pN0)</i> <input type="checkbox"/> Present [pN0 (+)]
Lymphovascular invasion^a <input type="checkbox"/> Not identified <input type="checkbox"/> Present
Venous invasion^b <i>Applied when identified in large vessels with an identifiable smooth muscle layer or elastic lamina</i> <input type="checkbox"/> Not identified <input type="checkbox"/> Present
Perineural invasion^a <input type="checkbox"/> Not identified <input type="checkbox"/> Present
Pre-existing adenoma^a (when present) <i>Used if the carcinoma is within the adenoma</i> <input type="checkbox"/> Tubular/Tubulovillous/Villous adenoma <input type="checkbox"/> Low grade dysplasia/High grade dysplasia
Associated findings^a (when present) <input type="checkbox"/> Tumor perforation <input type="checkbox"/> Serosal (peritoneal, mesenteric) seeding <input type="checkbox"/> Distant metastasis Other organ, specify: _____ Distant lymph node
Separate lesions^a (when present) <input type="checkbox"/> Peptic ulcer <input type="checkbox"/> Adenoma <input type="checkbox"/> GIST <input type="checkbox"/> Others (_____)

EGC, early gastric cancer; AGC, advanced gastric cancer; WHO, World Health Organization; EGJ, esophagogastric junction.

^aStandard data elements; ^bConditional data elements.

multiple lesions. Multiple lesions should be evaluated individually both macroscopically and microscopically in descending order from the tumor with the deepest level of invasion. However, regional lymph node metastasis, associated findings, and separate lesions are listed only for the deepest lesion.

Tumor location

The description of the tumor location is recorded in two parts: involvement and center. The *involvement* of the tumor uses up to three portions from the esophagus to duodenum beginning with the most involved area. The delineation of the upper, middle, and lower thirds of the stomach follows the Japanese guideline [9].

The *center* of the tumor is described using a combination of locations according to the International Classification of Diseases for Oncology classification [10] (cardia, fundus, body, antrum, pylorus, lesser curvature, greater curvature) plus the anterior wall and posterior wall [11]. If none of those options appropriately describes the location of the tumor, other can be used.

Tumor size

The tumor size is recorded using the largest dimension of the tumor [11]. Secondary or tertiary dimensions can be measured as conditional data elements. However, the tumor size is not used in the current staging of GC [8], and it is sometimes very difficult to

Table 2. Report form for pathologic diagnosis using endoscopic resection specimens

Standard and Conditional data elements
Specimen size^a <input type="checkbox"/> ___ x ___ cm
Gross type of tumor^a <i>Same as method of surgical specimen</i>
Tumor size^a <i>One largest dimension</i> <input type="checkbox"/> ___ cm
Histologic type^a <i>According to the principles described in "Histologic classification" section</i> <input type="checkbox"/> WHO <input type="checkbox"/> Lauren
Histologic components^b <i>All morphologic components of tumor cell may be described</i>
Depth of invasion (pT)^a <input type="checkbox"/> Invades lamina propria (pT1a) <input type="checkbox"/> Invades muscularis mucosae (pT1a) <input type="checkbox"/> Invades submucosa (submucosal depth: ___ mm or μ m) <input type="checkbox"/> Invades proper muscle (pT2)
Depth of invasion (pT)^b <i>In case of submucosa invasion, the invasion width can be additionally described</i> <input type="checkbox"/> invades submucosa (submucosal depth: ___ mm or μ m) (submucosal width: ___ mm)
Resection margin^a <input type="checkbox"/> Lateral margin <input type="checkbox"/> Free from carcinoma (safety margin, ___ cm) <input type="checkbox"/> Involved by carcinoma <input type="checkbox"/> Deep margin <input type="checkbox"/> Free from carcinoma (safety margin, ___ cm) <input type="checkbox"/> Involved by carcinoma
Resection margin^b <input type="checkbox"/> Proximal margin <input type="checkbox"/> Free from carcinoma (safety margin, ___ cm) <input type="checkbox"/> Involved by carcinoma <input type="checkbox"/> Distal margin <input type="checkbox"/> Free from carcinoma (safety margin, ___ cm) <input type="checkbox"/> Involved by carcinoma <input type="checkbox"/> Anterior margin <input type="checkbox"/> Free from carcinoma (safety margin, ___ cm) <input type="checkbox"/> Involved by carcinoma <input type="checkbox"/> Posterior margin <input type="checkbox"/> Free from carcinoma (safety margin, ___ cm) <input type="checkbox"/> Involved by carcinoma <input type="checkbox"/> Deep margin <input type="checkbox"/> Free from carcinoma (safety margin, ___ cm) <input type="checkbox"/> Involved by carcinoma
Ulceration^a <input type="checkbox"/> Absent <input type="checkbox"/> Present
Ulceration^b <input type="checkbox"/> Absent <input type="checkbox"/> Non-significant (≤ 4 mm) <input type="checkbox"/> Significant (> 4 mm)
Cases with adenoma components^a <input type="checkbox"/> Absent <input type="checkbox"/> Present specify: _____
En bloc resection^a <input type="checkbox"/> Yes <input type="checkbox"/> No (piecemeal/tearing)
Lymphatic invasion^a <input type="checkbox"/> Not identified <input type="checkbox"/> Present
Venous invasion^a <input type="checkbox"/> Not identified <input type="checkbox"/> Present

WHO, World Health Organization.

^aStandard data elements; ^bConditional data elements.

measure accurately, such as in Borrmann type 4 cancer. For scattered residual tumor foci following previous treatment, it is recommended to measure the maximum diameter that includes all foci [12].

Tumor regression grade

Although preoperative chemotherapy has not been established as a standard treatment for patients in Korea [5], studies have shown survival benefits in local AGC in European [13], Asian [14], and Korean patients [15]. Therefore, the need to adequately evaluate the tumor response to chemotherapy is increasing [16]. Various tumor regression grading (TRG) methods are available for gastrointestinal cancers [17,18]. The Becker system [19] is one that has been proposed for GC. The previous edition of "A Standardized Pathology Report for Gastric Cancer" [3] used the Japanese guideline [9]. The Becker and Japanese systems both estimate the proportion of residual tumor and use it as a cutoff value between TRGs. However, because some tumors have more abundant fibrosis than tumor cells (before chemotherapy), estimation of the residual tumor proportion could show low concordance between observers [20,21]. Therefore, we suggest a new TRG system: the modified Ryan system currently recommended in the College of American Pathologists (CAP) guideline [11] and the second edition of the standardized pathology report for colorectal cancer in Korea [22]. It is a descriptive four-tier system that evaluates residual cancer rather than fibrosis as none, single cells or rare small groups, more than single cells but evident tumor response, and extensive residual cancer cells. Acellular mucin pools and necrotic or degenerative cells are not considered to be residual cancer [8]. Only the primary tumor is evaluated in this TRG, but tumor regression of the regional lymph nodes [16,23] can be reported as a conditional data element when there is evidence of partial (viable cancer cells with regressive changes) or complete tumor regression (only fibrosis, mucin pool, or foam cells without viable cells) in the regional lymph nodes. Evidence suggests that the presence of tumor regression in the lymph nodes is associated with better clinical outcomes [24,25].

Depth of invasion

The depth of the tumor invasion follows the AJCC 8th edition [8] and Japanese guidelines [9]. Notably, the Japanese guideline does not accept carcinoma *in situ* (pTis). In the AJCC 8th edition, pTis is defined as an intraepithelial tumor without invasion of the lamina propria, which is equivalent to high-grade dysplasia. pT1b is subdivided into sm1, sm2, and sm3. If cancer cells are present below an imaginary line dividing the submucosa and

proper muscle, the case is considered pT2 even if the cancer cells are not actually within the muscle fibers. If there is no proper muscle layer due to ulceration, and the cancer cells are below the imaginary line drawn at the lower border of the proper muscle, the case is considered pT3. Invasion of the omentum and perigastric fat is considered pT3. Ink should be applied at the serosal surface nearest the tumor during gross examination to properly evaluate serosal (visceral peritoneum) invasion. The case is considered pT4a if the cancer cells are adherent to or exposed beyond mesothelial cells. Because the mesocolon and gastric serosa (including the greater and lesser omentum) have different embryological origins, invasion of the mesocolon should be classified as pT4b. However, some areas are tightly fused, such as the posterior wall of the antrum, the gastric serosa, and the anterior side of the transverse mesocolon. Therefore, the Japanese guideline indicates that invasion of the transverse mesocolon is not pT4b unless it extends to the colic vessels or penetrates the posterior surface of the mesocolon [9]. Some cases can be either pT4a or pT4b, depending on the site of the tumor. Invasion of the pancreas capsule is considered pT4b. Direct duodenal or esophageal invasion is not considered pT4b. Any involvement of other organs, such as the liver, pancreas, colon, spleen, diaphragm, or kidney, should be recorded. Cancer cells within lymphatic or vascular spaces are not considered in the determination of invasion depth [8]. The presence of lymphatic or vascular invasion should be recorded separately in parentheses (e.g., tumor invades proper muscle [involvement of subserosa by lymphatic emboli]).

Resection margin

The distance from the proximal or distal resection margin is the length from the edge of the carcinoma to the nearest resection margin. It is important to locate the true resection margin in the gross specimen, especially when the stomach is opened along the lesser curvature or obliquely along the anterior or posterior wall. In some cases, cancer cells approach the resection margin much more closely than can be observed grossly (cancer spreading underneath the mucosa). Therefore, the resection margin is finalized in a microscopic evaluation. The circumferential and radial resection margin statuses can be reported as conditional data elements. Determination of the circumferential margin is often required if the tumor is located near the EGJ.

Regional lymph node metastasis

The presence of lymph node metastasis is one of the most important prognostic factors, even post-chemotherapy [26,27]. Both the total number of evaluated lymph nodes and the number of

metastatic lymph nodes are reported. Although pathological evaluation of more than 30 regional lymph nodes is desirable according to the AJCC 8th edition [8], a minimum of 16 regional lymph nodes is acceptable per the CAP guideline [11] because the definition of pN3b is 16 or more metastases. Therefore, if fewer than 16 lymph nodes were initially retrieved for evaluation, additional effort to recover more lymph nodes should be made and reported. This does not apply in cases of previous partial gastrectomy, preoperative chemotherapy, or radiation therapy. Microscopic evaluation should be performed on the largest plane of each lymph node. In general, if the size of the metastasis observed in the lymph node is ≤ 0.2 mm, the metastasis is called isolated tumor cells (ITCs); if the size is more than 0.2 mm but not greater than 2 mm, it is a micrometastasis. Because micrometastases are not reported separately in GC, they are considered to be positive lymph nodes [8]. According to the AJCC 8th edition, ITCs should not be reflected in the pN stage and should be reported as pN0 (i+) in the absence of another lymph node metastasis. However, it is hard to ignore ITCs, which are readily seen on hematoxylin and eosin (H&E) slides. Therefore, in most practices, all metastatic tumor cell clusters in the lymph nodes are reflected in the pN stage regardless of size, and only ITCs incidentally detected by cytokeratin immunohistochemistry (IHC) are excluded from the pN stage. The stations of the lymph nodes are not reported unless they are separately submitted with corresponding labels. Tumor deposit (TD) is defined as discrete tumor nodules separate from the tumor bed (within the lymphatic drainage of the primary tumor) without identifiable lymph node tissue or vascular or neural structure (Fig. 1) [8]. Unlike colorectal carcinoma, TDs are considered to be metastatic lymph nodes in

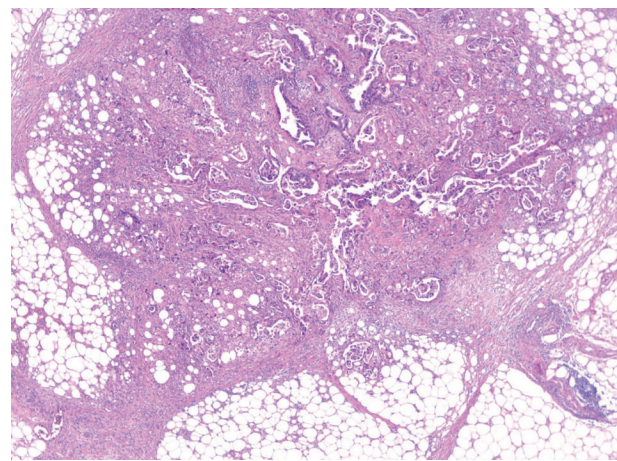


Fig. 1. An example of a tumor deposit. It usually has irregular outlines without identifiable lymph node tissue or identifiable vascular or neural structures.

GC and are thus reflected in the pN stage. TD and serosal (peritoneal) seeding nodules should be distinguished because peritoneal seeding is graded as pM1. Metastasis to a distant lymph node is pM1 and should not be considered in the pN stage. The definition of distant lymph nodes is different in the AJCC 8th edition than in the Japanese guideline, and we recommend following the AJCC 8th edition, in which superior mesenteric lymph node metastasis is pM1 [8].

Extranodal tumor extension

If the cancer cells show infiltration of the extranodal adipose tissue beyond the capsule of the lymph node, extranodal tumor extension (ENE) can be reported. ENE is associated with poor prognosis in GC [28-30].

Lymphovascular invasion

Lymphovascular invasion includes both lymphatic and vascular invasion. Discrimination of lymphatics from blood vessels on H&E slides is often difficult, especially when they are small (Fig. 2A, B). Although IHC for D2-40 or CD31 can be used, the prognostic differences between lymphatic and blood vessel invasion have not been sufficiently evaluated in GC [12]; therefore, we recommend using 'lymphovascular invasion.' However, when tumor invasion or emboli are observed in large vessels with an identifiable smooth muscle layer or elastic lamina, it is called venous invasion and can be reported as a conditional data element (Fig. 2C). Venous invasion has been reported as a risk factor for recurrence in both early [31,32] and advanced GCs [33].

Perineural invasion

Perineural invasion is reported when cancer cells are observed within or around the nerve [34].

Pre-existing adenoma

Pre-existing adenoma is reported when carcinoma is observed within an adenoma. If the adenoma is discrete from the carcinoma,

it is reported as a separate lesion.

Associated findings

Tumor perforation, serosal (peritoneal, mesenteric) seeding, and distant metastasis (including specific site) are reported when present.

Separate lesions

Peptic ulcers, adenomas, gastrointestinal stromal tumors, and other separate lesions are reported when present.

Endoscopic resection specimens

Description of the specimen

The size of the specimen is expressed as the length of the longest axis and the length perpendicular to the longest axis. The size of the tumor is indicated only by the length of the largest axis. The gross type of the tumor is described in the same way as for a surgical specimen.

Sectioning of the specimen

Apply ink to the entire deep margin and lateral margins of the specimen so that it can be viewed under a microscope. Prepare paraffin blocks by sequential parallel sectioning of the entire specimen at 2 mm intervals. Among the lateral margins of the four directions, the closest margin and the tumor should be included together in the sectioning direction.

For gastrointestinal specimens, the distal part is generally placed at the 9 o'clock position in a gross photograph. If the distances from each of the lateral margins are similar, serial sectioning of the specimen is commonly performed in the same direction. When visual observation indicates that the closest lateral margin is not included in this general sectioning direction, however, the direction of the sample or mapping frame should be turned so that the closest lateral margin and the tumor appear together on the section (Fig. 3).

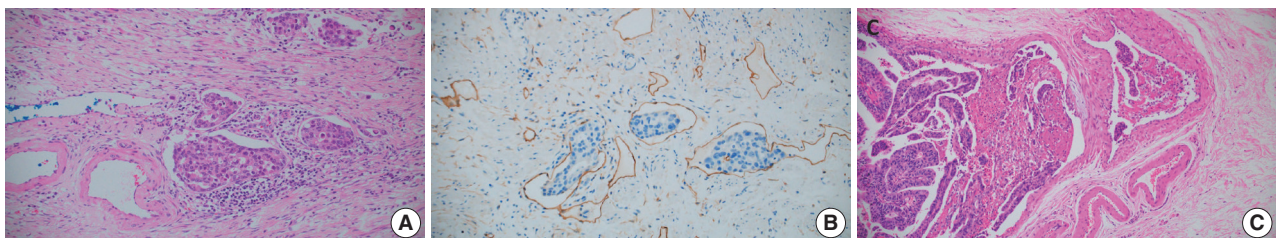


Fig. 2. Histologic features of lymphovascular invasion in sections of gastric cancer. An example of lymphovascular invasion on hematoxylin and eosin examination (A) and stained for D2-40 (B). Tumors involving vessels with an identifiable smooth muscle layer are considered to have venous invasion (C).

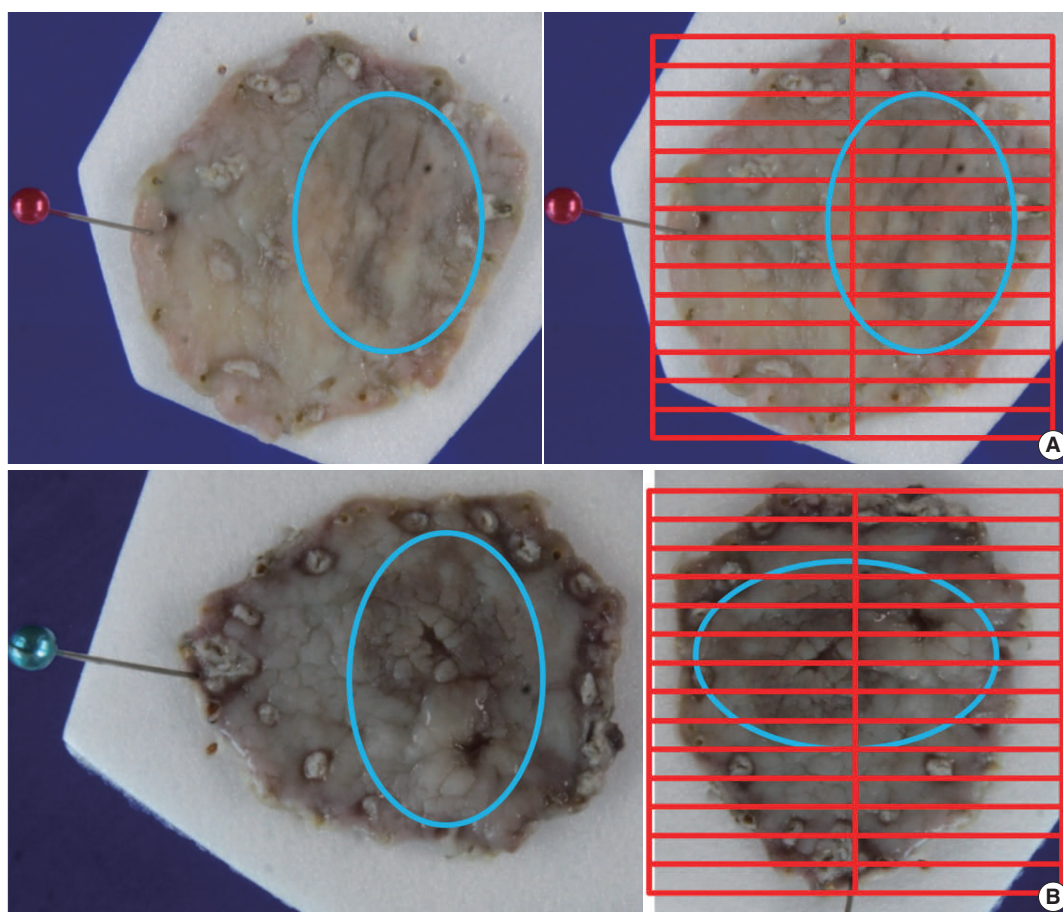


Fig. 3. Sectioning of an endoscopically resected specimen. When the direction of the photograph matches the direction of the closest lateral margin (A). If the direction of the photograph does not match, turn the specimen toward the closest lateral margin for mapping (B).

Histologic type and components

The histologic type of the tumor is described in the same way as for a surgical specimen. For the criteria and description of each type, refer to the information in the “Histologic classification” section below. The histologic type of the tumor should be described; the histologic diversity of tumor cells may be described separately as histologic components. If various morphologic components are observed within the tumor, all are described according to the histologic type. In such a case, the description should signify the quantitative majority of the tumor components. The description method can be selected according to institutional preferences. For example, record in order: well differentiated (WD)–moderately differentiated (MD) > poorly differentiated (PD) > signet ring cell (SRC) carcinoma; interval variable: WD-MD > 50%, PD < 50%, SRC < 10%; and continuous variable: WD-MD 65%, PD 30%, SRC 5%. Many studies have reported that tumors with a mixture of differentiated-type and undifferentiated-type components have a higher risk of lymph node metastasis than tu-

ors with only one component [35–40]. Within the undifferentiated type, SRC has a lower lymph node metastasis frequency, which is reported to be at a level similar to that of the differentiated type [41–43]. In addition, some reports indicate that the lymph node metastasis frequency is lower in pure SRC cases than in SRC cases mixed with other component types [44–47]. However, only the histologic type is applied for determining whether an endoscopic resection is curative, and because differences in histologic components are not applied, they are reflected as conditional elements rather than a standard element. A pathological study of the criteria for determining whether an endoscopic resection is curative is currently underway by the GIPSG of the Korean Society of Pathology as a research project of the National Evidence-based Healthcare Collaborating Agency. If important results are obtained from that study, they should be reflected in the elements of this guideline.

Tumor size

Only the length of the largest axis of a histologically confirmed tumor is recorded.

Depth of invasion

The method for describing the depth of invasion is basically the same as for a surgical specimen. The difference is that the invasion depth in the submucosal layer is measured and described in cases of submucosal invasion, and it is measured in mm or μm . The measurement is the length from the lowest surface of the muscularis mucosae to the most deeply invaded point. In some cases, the muscularis mucosae are modified by tumor invasion (hypertrophied, displaced, completely disappeared). In these cases, depth is measured using an imaginary line extending from adjacent muscularis mucosae in the normal area not deformed by the tumor (Fig. 4A). Always ensure that the lowest surface of the original, unmodified muscularis mucosae is used as the reference point. If the progressing course of the adjacent muscularis mucosae forms a curve, the virtual line is set as a matching curve (Fig. 4B).

No definitive description or research results indicate how to measure the depth of invasion when muscularis mucosae are modified. In the Japanese guideline, an explanation first appeared in the 14th edition from 2010: “if the muscularis mucosae are obscure due to ulcerative changes, the length should be measured on the virtual line based on the adjacent normal layer” [9]. In the

15th edition from 2017, it changed to recommend measuring from the surface of the tumor [48]. When muscularis mucosae are modified, some Korean pathologists measure from the lowest muscle fiber of the modified layer, and some measure from the imaginary line of the adjacent normal area. Two Korean studies reported that it is appropriate to measure from the imaginary line of the adjacent normal area in all modified situations [49,50]; accordingly, we use that recommendation as the standard measurement method in this guideline.

In cases of submucosal invasion, studies have shown that not only the invasion depth, but also the invasion width are significant risk factors for lymph node metastasis [50,51]. However, because few multicenter studies have been done and it has not yet been applied to the curative resection criteria, the invasion width is a conditional data element. This point is being addressed in the ongoing GIPSG pathological study on the criteria for determining whether an endoscopic resection is curative. The method for measuring the invasion width is as follows (Fig. 5): if submucosal invasion is observed on only one section, write the actual size measured on the slide of that section. If submucosal invasion is observed across two or more slices, write the larger of the following two values: (1) the actual size measured on the slide with the largest invasion width, or (2) the number of slices spanned by the invasion \times 2 mm (thickness of slice).

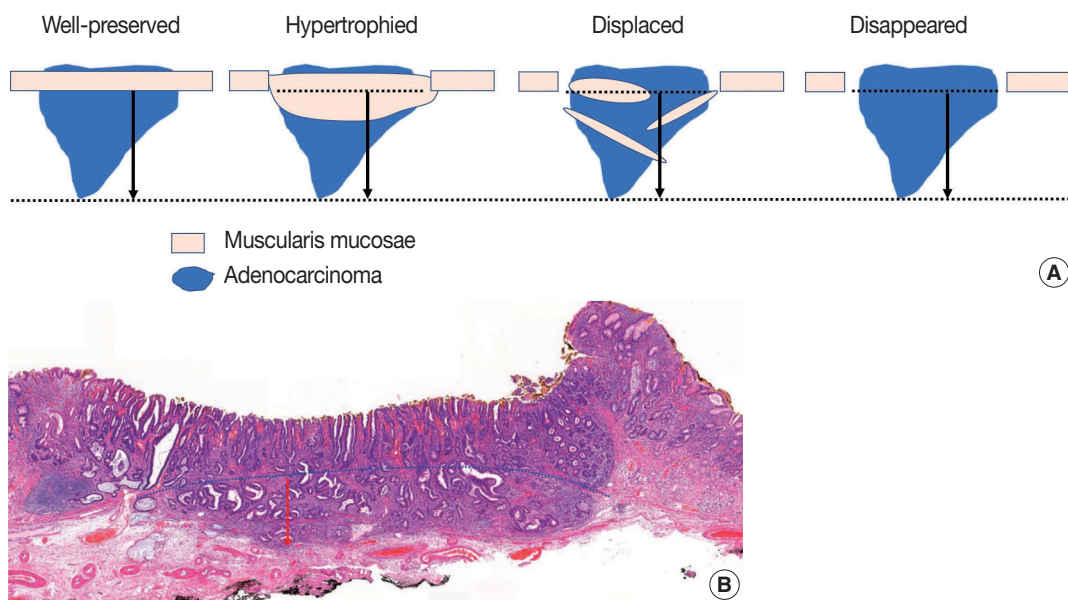


Fig. 4. Method to measure submucosal invasion depth. Always use the lowest surface of the original, unmodified muscularis mucosae as the reference point (A). When the progressing course of the adjacent muscularis mucosae forms a curve, the virtual line is set as a matching curve (B).

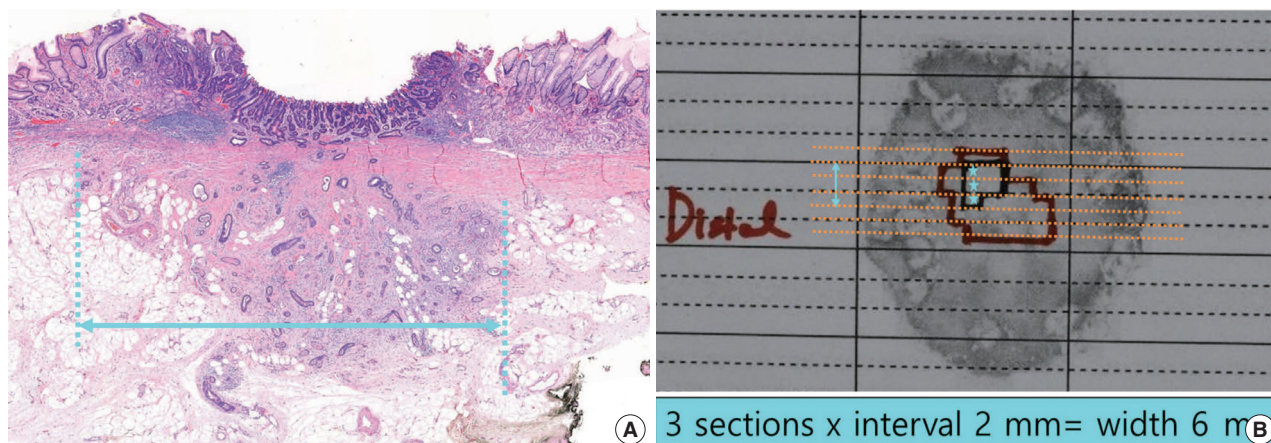


Fig. 5. Method to measure submucosal invasion width. The actual size measured within the slide (A). Number of slices that the invasion spans $\times 2$ mm (thickness of slice) (B).

Resection margin

The resection margin is described for the nearest lateral margin and deep margin. If the lateral margin is close (≤ 0.2 cm) or is involved in the tumor, the corresponding directions should be written together. If multiple margins are involved, all should be written. This is the information needed by the gastroenterologist to decide whether to perform additional procedures (endoscopic resection, argon plasma coagulation, follow-up biopsy). As a conditional element, the distance in all four directions of the lateral margin can be described.

The degree of invasion of the lateral resection margin and the probability of residual cancer are related. A high risk of residual cancer was reported when two or more of the four lateral margins were involved (multiple involvement) or when the length of involvement was large (more than 4 mm or 6 mm). However, it has not been determined whether additional treatment can be decided according to the degree of margin involvement because the risk is low but present in the group with a small degree of margin involvement.

Ulcer

Ulceration is defined as a full-thickness disruption of muscularis mucosae, both active and scarring, and determined by histological findings, not endoscopic findings [5,9,52]. The presence or absence of an ulcer is an important criterion for judging whether an endoscopic resection is curative in mucosal cancer [5], so it must be described in the pathology report for mucosal cancer. Because ulcers are included in the indications for an endoscopic resection, the presence of ulcers is determined by endoscopic findings. Ultimately, however, it must be confirmed by pathological examination findings of the resected specimen. En-

doscopic diagnosis is difficult in the absence of a mucosal break [53], and ulcer-negative endoscopy findings with ulcer-positive pathology findings were reported in 4.6%–5.5% of cases [54,55].

Another problem that occurs in practice is a lack of clarity in the criteria for differentiating original small ulcers from biopsy-induced changes after endoscopic biopsy in a case that did not originally have ulcers. Due to the low accuracy of ulcer determination in endoscopic findings, a finding of no ulcer during endoscopy cannot guarantee a biopsy-induced change. Diagnostic criteria for this have been suggested by Shimoda et al. [56], and the Japanese gastric cancer treatment guidelines describe this as follows: “A biopsy-derived scar is usually observed histologically as fibrosis restricted to small areas just beneath the muscularis mucosae. If it cannot be discriminated from the ulcer scar, it should be classified as UL1.” [57]. According to JCOG1009/1010, a clinical study on undifferentiated-type EGC: “UL was judged as present if the muscularis propria was completely disrupted and if fibrosis in the submucosal layer was observed to be wider than the range of disrupted muscularis propria.” [58]. In our study group, ulcer size was measured in the ongoing GIPSG study on the criteria for curative resection, and the possibility of offering differentiation criteria for this problem was investigated. We found that the risk of lymph node metastasis with an ulcer of 4 mm or less was the same as in cases with no ulcer. Using that criterion, very small ulcers can be excluded from the risk factors for lymph node metastasis, which removes the need to differentiate them from biopsy-induced changes. The grading of ulcer size is reflected as a conditional element. The method for measuring the size of an ulcer (Fig. 6) is similar to that used to measure the submucosal invasion width. If an ulcer (full-thickness disruption of the muscularis mucosae) is observed on only one section, write the

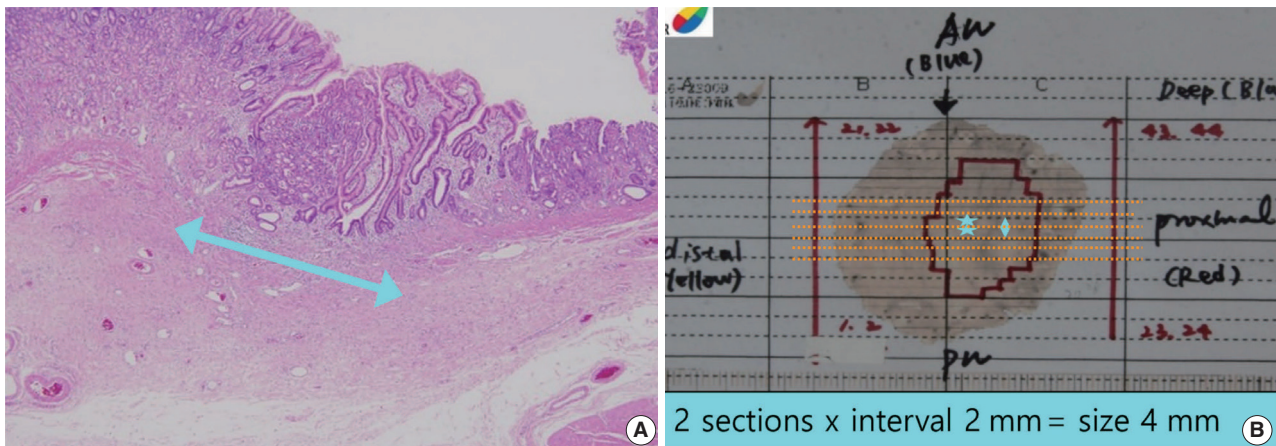


Fig. 6. Method to measure ulcer size. The actual size measured within the slide (arrow: ulcer size within the slide) (A). Number of slices that the ulcer spans $\times 2$ mm (thickness of slice) (star: ulcer-positive slices, arrow: slices that the ulcer spans) (B).

actual size measured on the slide. If it is observed across two or more slices, write the larger of the following two values: (1) the actual size measured on the slide with the largest disruption size or (2) the number of slices spanned by the disruption $\times 2$ mm (thickness of slice). The ulcer size is measured only within the tumor. If the ulcer spans the tumor and surrounding mucosa, measure the ulcer size only within the tumor area.

Cases with adenoma components

The adenoma component should be described only when the histological findings of adenoma are clear, and the intratumoral region is distinct from the adenocarcinoma component.

In diagnosis, only the adenocarcinoma contents should be described, and adenomas should be described separately as an additional item. For the size of the tumor, the size of the adenocarcinoma is described first, followed by the size of the total tumor. The distance from the resection margin describes the closest distance to any tumor component. If the resection margin is involved in a tumor or is less than 0.2 cm, the component should be described.

Unlike colorectal cancer, GC occurs in the adenoma-adenocarcinoma pathway in only a small number of cases, and adenocarcinomas of very small size are common. In addition, in many cases of WD adenocarcinoma, structural abnormalities are not severe, so areas that are difficult to differentiate from adenoma can be mixed in the tumor. Therefore, a background adenoma is identified only when the histological findings are clear and the area within the tumor is distinct from the adenocarcinoma component. If it is difficult to distinguish the mixed components, the entire lesion is treated as an adenocarcinoma. For example, if one component corresponds to adenocarcinoma and another compo-

nent is severely dysplastic but difficult to determine as adenocarcinoma, the whole is treated as an adenocarcinoma component. For an adenoma, only the presence of the adenoma component is briefly described in a separate section.

En bloc resection

Piecemeal resection or full-thickness tearing should be confirmed and documented in the histological examination. Even if the specimen is resected into several pieces, it is not piecemeal if the tumor is intact within one piece.

Lymphatic/venous invasion

Unlike surgical specimens, lymphatic and venous invasions are recorded separately in endoscopic resection specimens because of the differing risks of lymph node metastasis. Both lymphatic invasion and venous invasion are criteria for determining a non-curative resection. However, the risk of lymph node metastasis posed by lymphatic invasion is times higher than that from venous invasion, and a higher score is assigned in the risk prediction model [59]. This information is helpful when clinicians decide whether or not to perform gastrectomy; thus, it is recommended to report them separately. The standard method for differentiating lymphatic and venous invasion is H&E staining with the following criteria: it is determined as a lymphatic vessel when there is a thin wall or lymphatic fluid and as a venous vessel when there is a thick muscle wall or many red blood cells in the lumen. When it is difficult to distinguish between lymphatic vessels and small venules, classify them as lymphatic vessels.

IHC staining may be performed to better observe lymphatic or venous vessels. However, because H&E and other immunostained slides are obtained from different levels, they should be

interpreted separately. A specimen is deemed to be positive even if invasion is observed on only one slide.

Histologic classification

Histologic classification of GC is based on the 5th edition of the World Health Organization (WHO) blue book [4]. Representative histopathologic types described in the WHO classification are summarized in Table 3 and Fig. 7. The diagnosis of GC is usually determined according to the component that occupies the largest portion of the tumor, but the diagnosis of special histologic subtypes is based on the diagnostic criteria of each subtype. The most common subtype is tubular adenocarcinoma, characterized by prominent dilated or slit-like tubules. Carcinomas composed of solid tumor clusters with rare tubule formation are also classified as tubular adenocarcinoma. Tumor cells can be columnar, cuboidal, or flat, and luminal mucin/cell debris is common.

Papillary adenocarcinoma shows a papillary tumor structure with a central fibrovascular core and columnar or cuboidal tumor cells. For a diagnosis of papillary adenocarcinoma, more than 50% of the tumor area must contain the papillary tumor component [60-62]. High rates of liver metastasis, lymphovascular invasion, lymph node metastasis, and poor prognosis are reported in papillary adenocarcinoma [61-64].

Mucinous adenocarcinoma is defined when more than 50% of the tumor area shows extracellular mucin. Tumor cells in mucinous adenocarcinoma can show a glandular growth pattern, solid pattern, or scattered single cell pattern, including SRC carcinoma-

ma [4]. Mucinous adenocarcinoma is classified as the intestinal, diffuse, or indeterminate type according to the main component of tumor cell differentiation [4]. Mucinous adenocarcinoma tends to be diagnosed at an advanced stage [65,66].

Poorly cohesive carcinoma (PCC) is the second most common subtype of GC and is composed of isolated or small groups of tumor cells without gland formation [4]. Until the 3rd edition of

Table 3. Histopathologic classification of gastric carcinoma

Histopathologic classification	
WHO classification	
<input type="checkbox"/>	Tubular adenocarcinoma
<input type="checkbox"/>	Tubular adenocarcinoma, well differentiated
<input type="checkbox"/>	Tubular adenocarcinoma, moderately differentiated
<input type="checkbox"/>	Tubular adenocarcinoma, poorly differentiated
<input type="checkbox"/>	Papillary adenocarcinoma
<input type="checkbox"/>	Mucinous adenocarcinoma
<input type="checkbox"/>	Poorly cohesive carcinoma
<input type="checkbox"/>	Poorly cohesive carcinoma, signet-ring cell type
<input type="checkbox"/>	Poorly cohesive carcinoma, not otherwise specified
<input type="checkbox"/>	Mixed adenocarcinoma
<input type="checkbox"/>	Adenocarcinoma with lymphoid stroma
<input type="checkbox"/>	Hepatoid adenocarcinoma
<input type="checkbox"/>	Micropapillary adenocarcinoma
<input type="checkbox"/>	Adenocarcinoma of fundic-gland type
<input type="checkbox"/>	Undifferentiated carcinoma
<input type="checkbox"/>	Squamous cell carcinoma
<input type="checkbox"/>	Adenosquamous carcinoma
<input type="checkbox"/>	Gastroblastoma
<input type="checkbox"/>	Others (specify: _____)
Lauren classification	
<input type="checkbox"/>	Intestinal
<input type="checkbox"/>	Diffuse
<input type="checkbox"/>	Indeterminate
<input type="checkbox"/>	Mixed

WHO, World Health Organization.

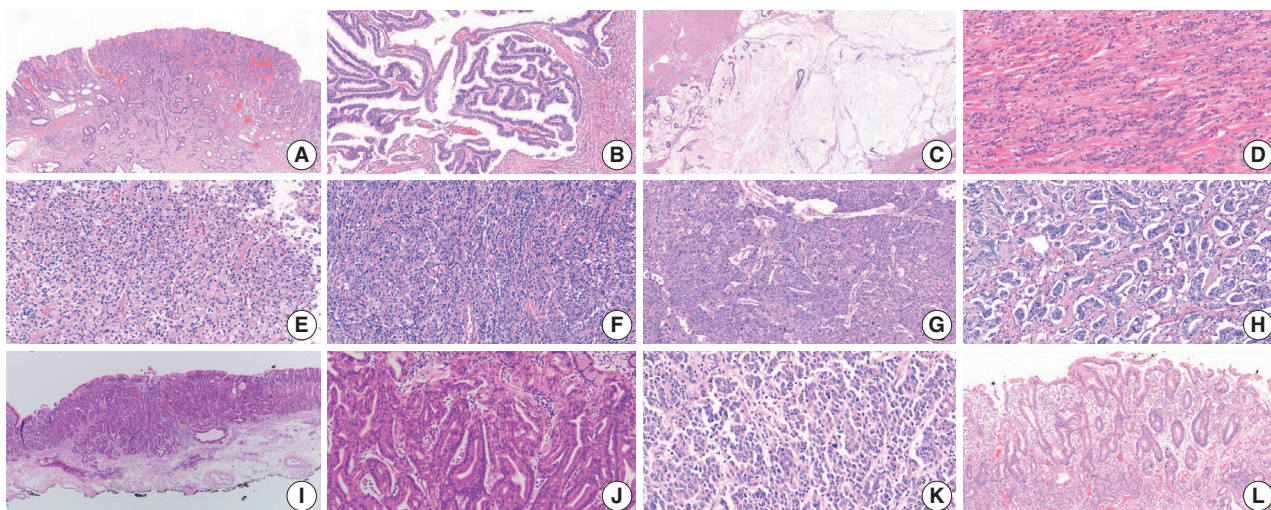


Fig. 7. Representative pictures of each histologic subtype of gastric carcinoma. Tubular adenocarcinoma (A), papillary adenocarcinoma (B), mucinous adenocarcinoma (C), poorly cohesive carcinoma, not otherwise specified (D), poorly cohesive carcinoma, signet-ring cell type (E), adenocarcinoma with lymphoid stroma (F), hepatoid adenocarcinoma (G), micropapillary adenocarcinoma (H), adenocarcinoma of the fundic-gland type (I, J), undifferentiated carcinoma (K), and crawling-type adenocarcinoma (L).

the WHO classification, SRC carcinoma was an independent subtype, but since the 4th edition of WHO classification, SRC has been included in the PCC category. Recently, several studies have suggested that non-SRC PCC (PCC-NOS) has a relatively poor prognosis compared with SRC and that SRC and PCC-NOS have different molecular profiles [67-70]. The WHO classification defines SRC as “composed predominantly or exclusively of signet-ring cell components” [4]. A European group suggested a PCC classification definition according to the percentage of the SRC component (SRC, > 90%; PCC-NOS, < 10%; PCC with SRC component, 10%–90%), but no definite criteria for diagnosing PCC-NOS and SRC have been established, so more studies are required [71].

Mixed adenocarcinomas, according to the WHO definition, are carcinomas with both glandular (tubular adenocarcinoma/papillary adenocarcinoma) and poorly cohesive (PCC/SRC) components [4]. Some reports recently suggested that mixed adenocarcinomas have poorer prognosis, such as frequent local recurrence and lymph node metastasis, than a pure subtype of carcinoma, especially in EGC [72,73]. However, no clear criteria have established a minimum ratio of glandular/poorly cohesive components for a diagnosis of mixed adenocarcinoma. Contrary to the WHO definition, many studies define mixed adenocarcinoma as PD adenocarcinoma or a PCC/SRC component mixed with gland-forming components; those studies also report that the prognosis of mixed adenocarcinoma in EGC is worse than that of pure subtypes [39,74,75]. Although mixed adenocarcinoma does not have a clear definition, it seems that EGC has a poor prognosis when a glandular component coexists with other components in the same tumor; therefore, when both a glandular component and other components are observed in an EGC, it is recommended that they be mentioned separately.

Adenocarcinoma with lymphoid stroma (medullary carcinoma with lymphoid stroma) was previously called ‘lymphoepithelioma-like carcinoma’ or ‘medullary carcinoma.’ Tumor cells of this subtype show irregular sheets, poorly defined clusters or tubules, trabeculae, or syncytial cells with dense lymphocytic infiltration and intraepithelial lymphocytes [4,76]. Such a tumor usually shows a well-defined margin without infiltrative growth and minimal desmoplasia. This type of tumor is frequently associated with Epstein-Barr virus (EBV) infection and sometimes shows microsatellite instability/mismatch repair deficiency [4,76]. Patients with this subtype show a lower number of lymph node metastases and better prognosis after surgery than those with other subtypes [77,78].

Hepatoid adenocarcinoma is composed of hepatocyte-like tu-

mor cells, which are large polygonal cells with eosinophilic-abundant cytoplasm arranged in a trabecular pattern [4,79]. This alpha-fetoprotein-positive tumor is often diagnosed preoperatively with multiple liver and lymph node metastases [4,79].

Micropapillary adenocarcinoma is characterized by an inside-out pattern of tumor clusters, which are small tumor clusters without a fibrovascular core, in clear spaces [4,80]. Micropapillary adenocarcinoma can be diagnosed when more than 10% of the tumor comprises micropapillary components [4,81]. This subtype is associated with poor prognosis and lymph node metastasis [4,80,81].

Adenocarcinoma of the fundic-gland type is composed of tumor cells showing chief cell differentiation, parietal cell differentiation, or both. Because this tumor does not show obvious nuclear dysplasia or structural abnormalities, it would be reasonable to regard it as adenocarcinoma only when it invades the submucosal layer. Lymph node metastasis is very rare in this subtype [4,82,83].

Undifferentiated carcinoma is composed of anaplastic cells without specific differentiation [4]. Grossly, a large ulcerating or fungating mass with necrosis is common. Tumor giant cells and rhabdoid tumor cells are common in this subtype, and spindle sarcomatoid cells can be seen [84,85]. Most patients show dismal prognosis with distant metastasis.

Squamous cell carcinoma is a very rare gastric tumor and shows morphology similar to that found in other organs. Adenosquamous carcinoma has both glandular and squamous tumor components, with $\geq 25\%$ squamous component [4]. Gastroblastoma is a biphasic tumor composed of spindle and epithelial cells.

Crawling-type adenocarcinomas are characterized by complex branching or anastomotic structures and low-grade nuclei and have not yet been classified as a distinct subtype in the WHO classification [4]. Because of their low-grade nuclear atypia, reactive looking structural change, and mucosal location, crawling-type adenocarcinomas were once called a very WD form of gastric adenocarcinoma. Recent studies have shown that large crawling-type adenocarcinomas are often accompanied by PD components, and one report indicates that lymph node metastasis occurs frequently when the cancer invades beyond the submucosal layer [86,87]. Although it has not yet been classified as a formal subtype, some research results on crawling-type adenocarcinoma have recently been published, and attention needs to be paid in terms of prognosis.

Tubular adenocarcinoma and papillary adenocarcinoma can be graded. When two or more differentiations are mixed in an adenocarcinoma, the differentiation grade reflects the largest tumor

area. A distinct glandular structure composed of columnar cells is classified as WD, and a small glandular structure composed of cuboidal or flat cells is classified as MD. In a tumor with an indistinct glandular structure, carcinoma forming frequent luminal structures is classified as MD, and that with a rare luminal structure is classified as PD (Fig. 8) [3]. Although the WHO recommends a two-tier grading system of low- (WD and MD) and high-grade (PD), most pathologists and clinicians use a three-tier grading system. We have agreed to use a three-tier grading system that can be easily switched to a two-tier grading system.

Histologic types in biopsy specimens

In endoscopic gastric biopsy samples, it is often difficult to diagnose a specific subtype of gastric carcinoma. However, histologic subtypes and differentiation are important in the selection of a treatment modality. We recommend reporting a histologic component or subtype if there is a PD component or subtypes associated with poor prognosis (such as PCC, PD tubular adenocarcinoma, or micropapillary feature), irrespective of the proportion. Some peculiar subtypes of adenocarcinomas, such as adenocarcinoma of the fundic-gland type and EBV-associated gastric carcinoma, have a lower rate of lymph node metastasis than other subtypes with similar invasion depth, especially in EGC [82,88,89]. Reporting these subtypes and testing for EBV in situ in biopsy specimens could thus be helpful for patient management [89].

Lauren classification

The Lauren classification has been one of the most commonly used classification systems for GC worldwide since its publication in 1965 (Table 3) [90]. According to the WHO 5th edition, WD and MD papillary adenocarcinoma and tubular adenocarcinoma are classified as the intestinal type, and PCC and SRC are classified as the diffuse type (Fig. 9). In the Lauren classification, the mixed type (not the same as mixed adenocarcinoma in the histological classification) is used when intestinal and diffuse

tumor components coexist in similar proportions. Although a table in the WHO blue book indicates that solid type, PD adenocarcinoma is classified as indeterminate type, this does not mean that all PD adenocarcinoma should be classified as such, and there is some disagreement among pathologists about the definition of the indeterminate type. Further discussion is needed to decide whether other special histological types of adenocarcinoma are excluded from the Lauren classification or whether they can be classified as intestinal, diffuse, or indeterminate according to their morphology.

To determine the feasibility of an endoscopic resection of tumors, most clinical guidelines and studies apply the differentiated type (papillary adenocarcinoma, tubular adenocarcinoma, WD and MD)/undifferentiated type (tubular adenocarcinoma, PD and poorly cohesive carcinoma, including SRC carcinoma) criteria of the Japanese guidelines [57]. In these criteria, PD adenocarcinoma is classified as the undifferentiated type. To prevent confusion with undifferentiated carcinoma, we do not recommend using the 'differentiated type/undifferentiated type' criteria in pathology reports. Instead, using the histologic classification and/or Lauren classification can provide sufficient information to clinicians and researchers.

Adenoma

Neoplastic epithelial proliferation without stromal invasion is called either adenoma or dysplasia. This intraepithelial neoplasia is usually called an adenoma by Western pathologists when the tumor shows a protruding, polypoid appearance with a distinct border and dysplasia when the tumor appears as a flat, depressed lesion or elevated indistinct lesion [4]. The Japanese classification tends to refer to elevated, flat, and depressed intraepithelial lesions as adenomas. Both adenoma and dysplasia can be used as terms for intraepithelial neoplasia in Korea.

Gastric adenomas can be subclassified into the intestinal type, foveolar type, pyloric gland type, and oxyntic gland type. Intestinal-type adenomas are the most common adenomas and usually

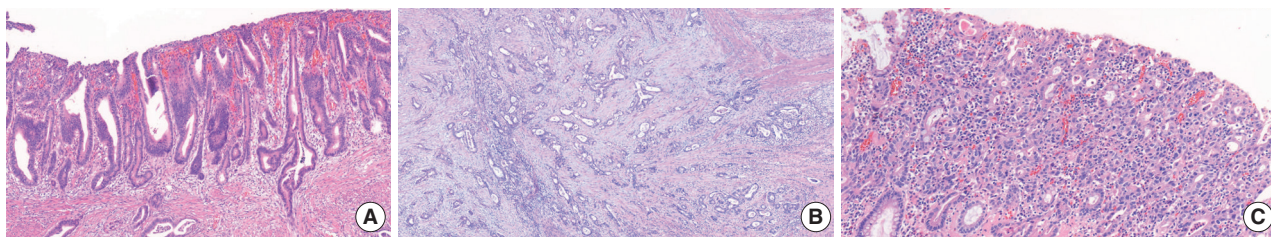


Fig. 8. Grading of gastric tubular adenocarcinoma. Well-differentiated adenocarcinoma showing glandular structures composed of columnar tumor cells (A). Moderately differentiated adenocarcinoma exhibits more complex tubular structures with cuboidal and/or flat epithelial cells (B). Tubular structure is unclear in most tumor glands in poorly differentiated adenocarcinoma (C).

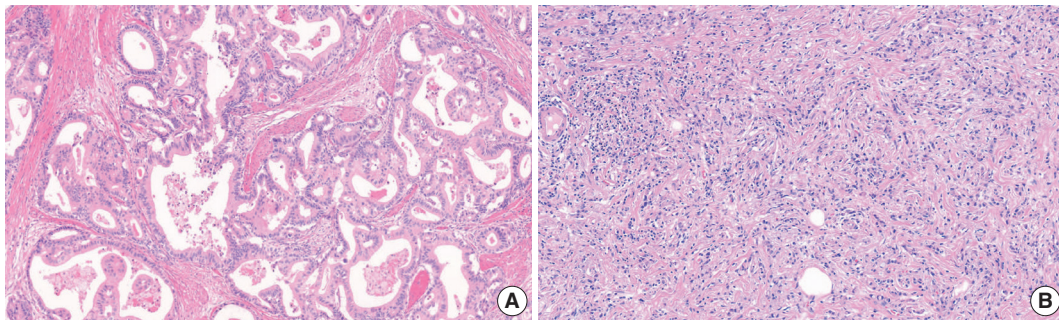


Fig. 9. Intestinal (A) and diffuse (B) Lauren type gastric adenocarcinomas characterized by well-formed tumor glands and interspersed tumor cells, respectively.

show tubule formation and columnar cells with elongated nuclei, with or without goblet cells and Paneth cells [4]. Foveolar-type adenomas are the second most common type of gastric adenoma, and an apical mucin cap is characteristic [91]. Pyloric gland type adenomas consist of columnar cells with ground-glass-like cytoplasm, basally located nuclei, and closely packed tubular glands with occasional dilatation [92]. Oxyntic gland type adenomas, also called oxyntic gland neoplasms because they can be diagnosed as adenocarcinoma only when submucosal invasion is confirmed, can progress into adenocarcinoma of the fundic gland type. This adenoma is composed of tumor cells with an oxyntic gland (chief cells, parietal cells, and mucous neck cells) and exhibits structural irregularity and minimal to mild nuclear atypia [82,88].

A two-tier system (low-grade/high-grade) is recommended for grading adenomas. Low-grade adenomas are characterized by a simple tubular or papillary architecture, hyperchromatic elongated or ovoid nuclei without severe atypia, preserved cellular polarity with basally located nuclei, and relatively regular intervening stroma without structural disruption. Goblet cells, apoptotic features, and mild to moderate mitotic features can be observed in low-grade adenomas (Fig. 10A). High-grade adenomas show more complex structures such as fusion, crowding, and budding of glands and the formation of glands with varying diameters. Cellular atypia is more pronounced in high-grade adenomas, such as loss of polarity, a high nuclear/cytoplasm ratio, pleomorphic nuclei, frequent mitosis, and atypical mitosis [93,94]. Intraglandular necrotic debris is also a diagnostic clue for high-grade dysplasia and, more commonly, adenocarcinoma (Fig. 10B) [95]. A diagnosis of adenocarcinoma should be considered when more than one of the following is present: evidence of stromal invasion (including single cell invasion into stroma and desmoplastic reaction), marked structural atypia, and marked glandular crowding (Fig. 10C) [94].

Helicobacter pylori

H. pylori infection is the most common cause of gastric adenocarcinoma, and eradication of *H. pylori* is associated with metachronous GC [96,97]. To detect *H. pylori* infection in a pathology specimen, additional staining (such as the Wright-Giemsa stain or Warthin-starry stain) is recommended. The proportion of drug-resistant *H. pylori* is increasing, and in patients with clarithromycin-resistant *H. pylori* infection, the failure rate of standard eradication treatment is also increasing. In patients with *H. pylori* infection, testing for clarithromycin-resistance is helpful for *H. pylori* eradication.

Molecular markers

All molecular tests are optional, conditional data elements. All report forms for the pathologic diagnosis of molecular markers are shown in Table 4.

Human epidermal growth factor receptor 2 testing

Determination of human epidermal growth factor receptor 2 (HER2) status is critical to identify patients with advanced-stage cancer for appropriate precision therapy. HER2-positive GC patients are currently treated with trastuzumab in combination with chemotherapy as first-line therapy, and fam-trastuzumab deruxtecan-nxki, a.k.a. trastuzumab deruxtecan, was recently approved by the Food and Drug Administration as a third- or later-line treatment [5,7,98,99]. HER2 status is principally determined by IHC or in situ hybridization (ISH) assays. HER2-positivity is defined as IHC 3+ or IHC 2+/ISH-positive [100,101]. HER2 testing requires formalin-fixed paraffin-embedded biopsy tissues with an adequate number of tumor fragments (ideally at least four) or representative surgical specimens with more differentiated components [102,103].

In currently recommended testing algorithms, HER2 status should be initially established using IHC [7,100] to estimate the

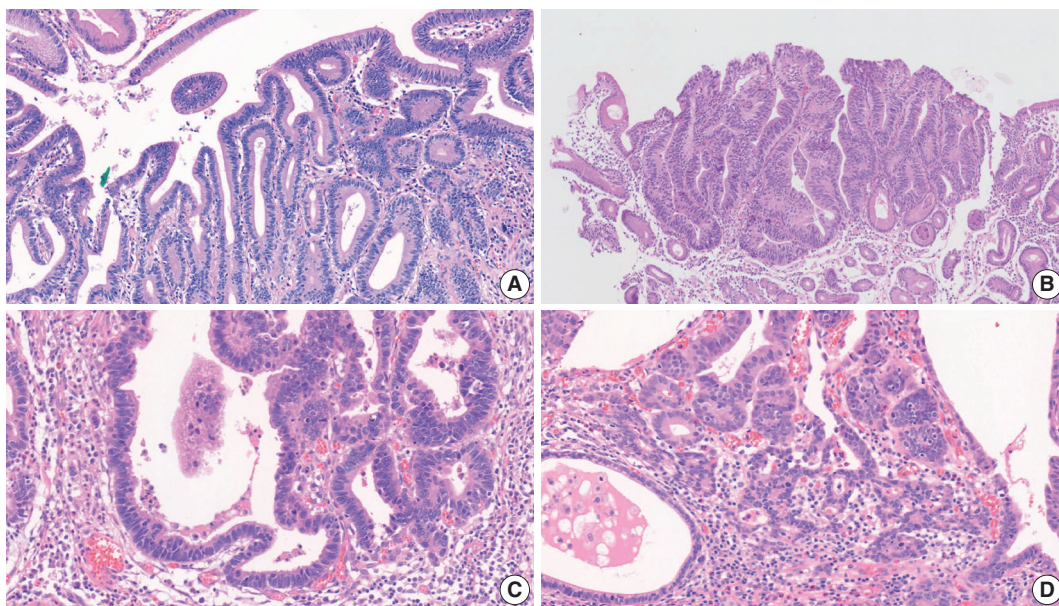


Fig. 10. Tubular adenoma with low-grade dysplasia shows simple tubular architecture composed of elongated tumor cells with preserved polarity (A). More crowding and variation in the size of the tumor glands are noted in high-grade adenoma (B). The diagnosis of adenocarcinoma can be made when tumor cells show single-cell infiltration into the lamina propria (C) and/or marked structural fusion and atypia (D).

immunoreactive intensity and percentage of basolateral membranous expression on cancer cells [7,104]. The score ranges from 0 to 3 based on $\geq 10\%$ cutoff level of HER2 expression in surgical specimens and ≥ 5 clustered cells in biopsy specimens as follows: 0 (negative), no reactivity or membranous reactivity in $< 10\%$ of cancer cells from surgical specimens or any cancer cells in biopsy specimens; 1+ (negative), faint or barely perceptible membrane reactivity; 2+ (equivocal), weak to moderate complete or basolateral membrane reactivity; and 3+ (positive), strong complete or basolateral membrane reactivity (Fig. 11).

Cases with a score of 2+ or indeterminate by IHC should be confirmed with ISH techniques to determine the final HER2 status [7,100]. Positive *HER2* amplification is defined as a *HER2*:CEP17 (centromeric region of chromosome 17) ratio ≥ 2.0 . To evaluate the ISH results, first check the HER2 IHC slide to select the most strongly stained region that might predict a higher level of *HER2* amplification. Next, at least 20 evaluable, non-overlapping invasive tumor cells should be counted. If CEP17 signals are ≥ 3 and the ratio of *HER2*:CEP17 is < 2.0 , an average *HER2* copy number > 6 signals/cell is considered positive for *HER2* amplification by ISH and < 4 signals/cell is considered negative. If an average *HER2* copy number is between four and six signals/cell, another 20 cells should be counted in a different area. Sometimes, the determination of HER2 status is uncertain due to sample problems or technical issues [103,105]. In that case, the test should be reported as “cannot be determined.”

Some studies have revealed a significant correlation between HER2 expression and histologic subtype in GC. The Trastuzumab for Gastric Cancer (ToGA) trial and other published studies showed that the HER2 positivity rate was higher in differentiated subtypes (Lauren intestinal type and WD and MD type) than in the Lauren diffuse type or PD type [106-108]. Furthermore, intratumor heterogeneity of HER2 expression was reported in approximately 50% of GC cases [106,109]. Inter-lesional heterogeneity of HER2 expression for either positive or negative shifting has been reported between primary carcinomas and synchronous or metachronous locoregional/distant metastases at a rate of 2%–14% [110-115].

Therefore, HER2 status should be re-evaluated for all newly diagnosed secondary, recurrent, and metastatic lesions, regardless of the HER2 status of the primary cancer because it affects the therapeutic strategy and prognosis of patients [116,117].

Microsatellite instability and mismatch repair deficiency

Microsatellites, also called short tandem repeats, consist of repeats of a sequence that ranges from 1–6 nucleotides in length [103,118,119]. DNA mismatch repair (MMR) is a highly conserved mechanism to recognize and replace or repair mismatched nucleotides during DNA replication [119]. MMR deficiency (dMMR) is commonly caused by a germline mutation or sporadic epigenetic silencing and leads to insertions or deletions of nucleotides in microsatellite regions during DNA replication [119,120].

Table 4. Report form for pathologic diagnosis using molecular markers

Molecular markers
<i>All molecular markers are "conditional data element"</i>
HER2 immunohistochemistry
<input type="checkbox"/> Negative (0/1+)
<input type="checkbox"/> Equivocal (2+)
<input type="checkbox"/> Positive (3+)
<input type="checkbox"/> Undetermined (explain):
HER2 (ERBB2) in situ hybridization
Number of invasive cancer cells counted: _____ cells
<input type="checkbox"/> Using dual-probe assay
<input type="checkbox"/> HER2 (ERBB2)/CEP17 ratio: _____
<input type="checkbox"/> Average number of HER2 (ERBB2) signals per cancer cell: _____
<input type="checkbox"/> Average number of CEP17 signals per cancer cell: _____
<input type="checkbox"/> Using single-probe assay
<input type="checkbox"/> Average number of HER2 (ERBB2) signals per cancer cell: _____
Summary: Negative/Positive for HER2 (ERBB2) gene amplification
<input type="checkbox"/> Undetermined (explain):
Microsatellite instability (MSI)
Summary:
<input type="checkbox"/> Microsatellite stable (MSS)
<input type="checkbox"/> Microsatellite instability-low (MSI-L)
<input type="checkbox"/> Microsatellite instability-high (MSI-H)
<input type="checkbox"/> Undetermined (explain) ^a
DNA mismatch repair immunohistochemistry
MLH1:
<input type="checkbox"/> Positive (retained expression)
<input type="checkbox"/> Negative (loss of expression)
<input type="checkbox"/> Undetermined (explain):
MSH2:
<input type="checkbox"/> Positive (retained expression)
<input type="checkbox"/> Negative (loss of expression)
<input type="checkbox"/> Undetermined (explain):
PMS2:
<input type="checkbox"/> Positive (retained expression)
<input type="checkbox"/> Negative (loss of expression)
<input type="checkbox"/> Undetermined (explain):
MSH6:
<input type="checkbox"/> Positive (retained expression)
<input type="checkbox"/> Negative (loss of expression)
<input type="checkbox"/> Undetermined (explain):
Summary:
<input type="checkbox"/> DNA mismatch repair deficiency (was/was not) observed
<input type="checkbox"/> Because it is difficult to determine DNA mismatch repair deficiency, PCR-based testing and/or NGS for MSI is recommended.
In situ hybridization for Epstein-Barr virus–encoded small RNAs
<input type="checkbox"/> Positive [diffuse/heterogenous (focal and/or mixed intensity)] ^{b,c}
<input type="checkbox"/> Negative
Summary: Epstein-Barr virus–associated gastric carcinoma
PD-L1 immunohistochemistry
PD-L1 [Antibody (22C3 PharmDx/22C3 conc. Ventana/28-8 PharmDx/others: _____)]:
<input type="checkbox"/> CPS = _____

HER2, human epidermal growth factor receptor 2; CEP17, centromeric region of chromosome 17; MLH1, mutL homolog 1; MSH2, mutS homolog 2; PMS2, PMS1 homolog 2; MSH6, mutS homolog 6; PCR, polymerase chain reaction; NGS, next-generation sequencing; PD-L1, programmed death ligand 1; CPS, combined positive score.

^aBecause it is difficult to determine MSI status, mismatch repair immunohistochemistry and/or NGS is recommended; ^bChecking the signal pattern is optional; ^cThe term "Epstein-Barr virus–associated gastric carcinoma" applies to positive cases.

The four genes that play an important role in this process are mutL homolog 1 (*MLH1*), mutS homolog 2 (*MSH2*), mutS homolog 6 (*MSH6*), and PMS1 homolog 2 (*PMS2*) [103,119-121]. When MMR does not function normally, it is called microsatellite instability (MSI) [119,122].

MSI is the hallmark of Lynch syndrome and is found in many sporadic cancers [103,123]. MSI-high (MSI-H) is observed in 6.9%–22.7% of sporadic GC cases [124-127]. As a distinct molecular subtype, MSI-GC is characterized by the gastric CpG island methylator phenotype with *MLH1* silencing [124]. The clinical characteristics of MSI-GC are antrum (distal) locations, intestinal type of Lauren histology, early disease stage, and favorable prognosis [5,103,125,126]. Clinically, MSI is an actionable predictive biomarker for resistance to 5-fluorouracil-based adjuvant chemotherapy and indicates good suitability for immunotherapy [128-132]. For this reason, clinician requests for MSI and/or MMR test are increasing. In the National Comprehensive Cancer Network Guidelines for Gastric Cancer V.2.2022, universal MSI and MMR testing is recommended for all newly diagnosed GC patients, in accordance with the CAP DNA Mismatch Repair Biomarker Reporting Guidelines [100].

The three main methods used to detect MSI/dMMR are as follows: (1) polymerase chain reaction (PCR) amplification of microsatellite sequences; (2) IHC staining to determine the expression of the four MMR proteins MLH1, MSH2, MSH6, and PMS2; and (3) next-generation sequencing (NGS) [103,119,120,133]. Additionally, a new kit enables diagnosis of MSI according to the number of deleted base mutations by using a melting curve analysis with a peptide nucleic acid (PNA) probe [134].

PCR can compare the allelic position of the microsatellite locus in the tumor with that in normal tissue [103,120,133]. The National Cancer Institute recommends the so-called Bethesda Panel as reference [133,135]. This panel is composed of two mononucleotide repeats (BAT-25 and BAT-26) and three dinucleotide repeats (D2S123, D5S346, and D17S250) [22,103,133,135]. These regions are amplified in parallel using fluorescent PCR, and their sizes are assessed by capillary electrophoresis [133,136]. However, because the dinucleotide markers are less sensitive and specific than the mononucleotide markers [137], an alternative panel with five poly-A mononucleotide repeats (NR-21, NR-24, NR-27 [or Mono-27], BAT-25, and BAT-26) has also been suggested [22,103,119].

MSI-H is defined as instability of two or more of five microsatellite loci; MSI-low (MSI-L) is defined as instability of one site, and microsatellite stable (MSS) is defined as no instability at any site. Currently, clinical studies tend to categorize MSI-L and MSS

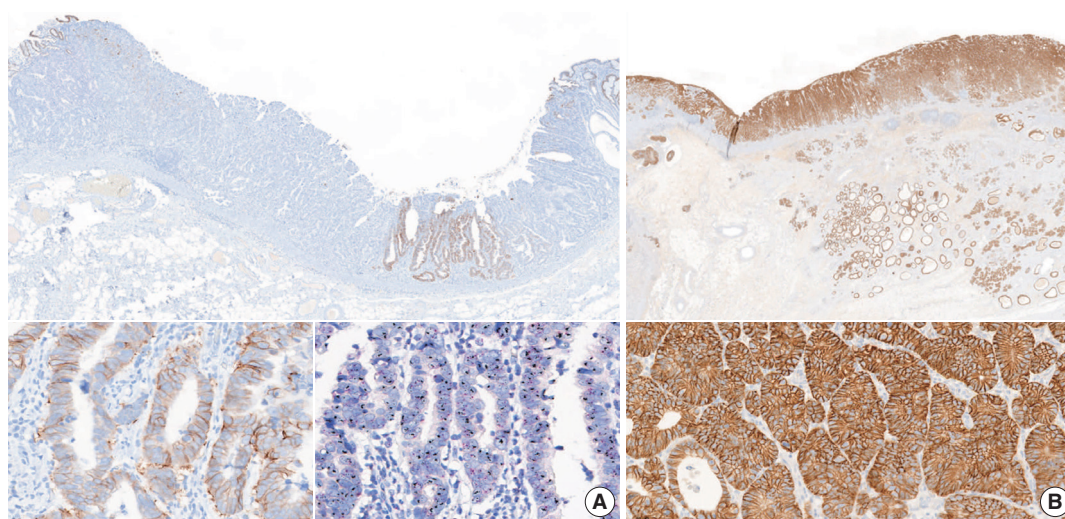


Fig. 11. Representative images of human epidermal growth factor receptor 2 (HER2)-positive gastric cancer. HER2 immunohistochemistry (IHC) of this case showed heterogeneous intratumoral expression, composed of some areas featuring a score of 2+ with *HER2* gene amplification and others scoring 0 (A). HER2 IHC of this case showed homogeneous HER2 positivity (score of 3+) (B).

as one type. This PCR method enables a functional measure of dMMR by directly measuring DNA changes. However, the method does not identify the MMR gene to be investigated. When the PCR test fails or the interpretation of the results is difficult, the test should be reported as “undetermined,” and IHC testing or NGS is recommended.

IHC for MMR proteins in GC samples is a simple and useful practice to determine dMMR. This method shows performance characteristics similar to MSI detection by PCR and a high concordance rate (> 90%) [138]. The use of all four proteins, MLH1, MSH2, MSH6, and PMS2, is recommended for the IHC test. However, in more than 90% of cases, MSI-GC is associated with MLH1 and/or PMS2 losses by hypermethylation of the *MLH1* gene. Because this IHC method is based on the ubiquitous expression of the MMR proteins in cell nuclei, nuclear staining should be checked when determining MMR positivity [22,119]. The presence of internal positive controls such as normal mucosa, lymphocytes, or stromal cells is essential for the interpretation of results [119]. dMMR is determined when the nuclear expression of at least one MMR protein is absent (Fig. 12) [22]. Heterogeneity of IHC or abnormal staining (cytoplasmic or membranous staining) is sometimes observed [138-143]. When it is difficult to interpret the IHC results, the test should be reported as “undetermined,” and PCR-based testing or NGS is recommended to confirm the MMR status. Using both IHC and PCR analyses for the detection of MSI-H/dMMR can reduce indeterminacy in the results.

EBV testing

EBV-associated gastric carcinoma belongs to one of four types of molecular classification suggested by the Cancer Genome Atlas (TCGA) [124]. Virus-host interactions play a pivotal role in EBV-induced carcinogenesis [144]. In EBV-associated gastric carcinoma, BamHI-A rightward frame 1 (*BARF1*) and latent membrane 2A (*LMP2A*) are putative viral oncogenes [145-147]. Once EBV enters the epithelium, EBV DNA methylation occurs globally. Hypermethylation of the CpG island promoter occurs throughout human cellular progress, which inactivates tumor suppressor genes [148]. Unique methylation leading to *CDKN2A* (p16) downregulation seems to be essential [124]. Eventually, EBV-infected gastric epithelial cells begin clonal growth, and gene mutations in EBV-infected cells lead to carcinogenesis [144]. EBV-associated gastric carcinoma is molecularly characterized by frequent mutations in phosphatidylinositol-4,5-bisphosphate 3-kinase catalytic subunit α (*PIK3CA*) [124] and AT-rich interaction domain 1A (*ARID1A*) [125], rare *TP53* mutations [124], and the overexpression of interferon- γ [149] and programmed death ligand 1 (PD-L1) [124,150].

EBV-associated gastric carcinoma has distinct histologic, genetic, and immune microenvironmental features. Notably, EBV-associated gastric carcinomas exhibit a dramatic response to pembrolizumab immunotherapy (100% overall response rate) [130]. EBV positivity can be a good indication for immunotherapy in GC. Moreover, in submucosal invasive GC, EBV positivity has been associated with a low risk of lymph node metastasis [151,152].

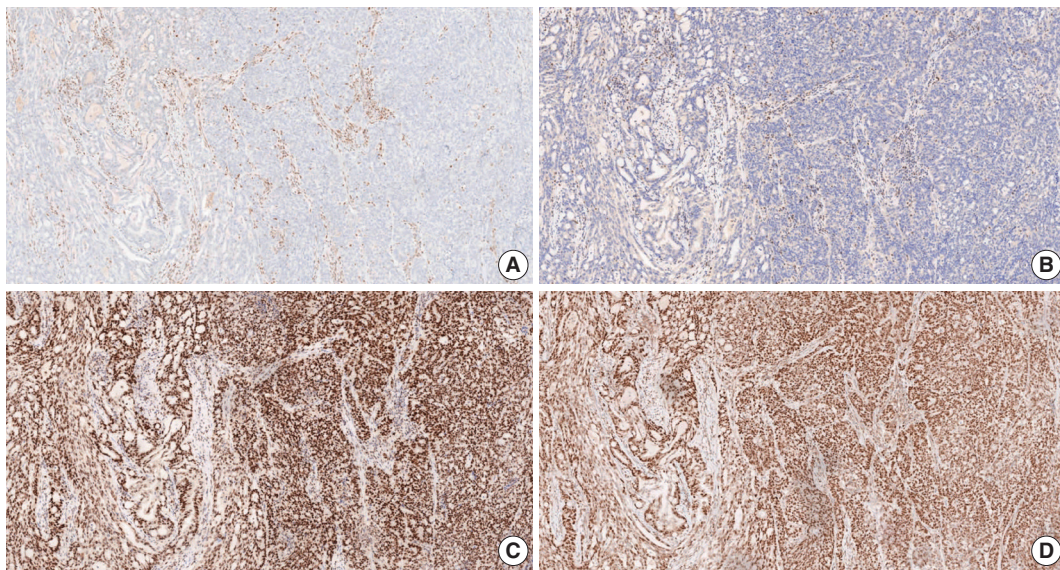


Fig. 12. A representative figure of gastric cancer with DNA mismatch repair deficiency. Immunohistochemistry for MLH1 (A) and PMS2 (B) showed loss of nuclear expression in tumor cells and positive nuclear expression in adjacent inflammatory cells. In contrast, immunohistochemistry for MSH2 (C) and MSH6 (D) showed retained nuclear expression in tumor cells. MLH, mutL homolog 1; PMS2, PMS1 homolog 2; MSH2, mutS homolog 2; MSH6, mutS homolog 6.

ISH for EBV-encoded small RNAs (EBERs) is the most suitable and widely used method to detect EBV in formalin-fixed paraffin-embedded tissues and cytology specimens [153,154]. It is a highly sensitive detection method because of the large number of EBERs (10^6 – 10^7 copies/cell) [19], but it cannot be used for quantitative analysis of viral particles. Several commercial probes for EBERs are available, in which EBERs labeled with biotin, digoxigenin, or fluorescein can be visualized by microscopic examination. In most EBV-associated GCs, EBER signals are observed with strong intensity in almost all cancer cell nuclei. In certain cases, EBER signals are heterogeneous, i.e., positive only in a focal portion of the cancer or mixed—weak to strong—intensity (Fig. 13). Recently, focal positivity of EBER signals was reported in 18% of EBV-associated GC cases in Germany [155]. In daily practice in Korea, however, intratumoral heterogeneity of EBER signals is not as high as in those German cases. Whether focal negative/weak intensity represents an absence of EBV infection or a subcritical or insufficient copy number of EBERs remains unclear [156]. EBER signals are rarely detected in intratumoral or peritumoral lymphocytes, which originate from peripheral B lymphocytes infected with EBV in a latent state.

PD-L1 immunohistochemistry

The programmed death-1 receptor (PD-1)–PD-L1 interaction is one of the major mechanisms of immune modulation that allow T-cell inactivation and tumor immune evasion [157].

Blocking the PD-1/PD-L1 pathway is a standard therapeutic strategy for various solid tumors, including GCs [158].

Pembrolizumab was granted accelerated FDA-approval as a third-line treatment of GC based on the findings of the phase 2 KEYNOTE-059 trial, which demonstrated its treatment benefit in advanced GC patients with PD-L1 combined positive score (CPS) positivity (CPS ≥ 1). Accompanying approval was granted for the PD-L1 IHC 22C3 pharmDx assay on the Autostainer Link 48 platform as a companion diagnostic assay [159]. However, the subsequent phase 3 KEYNOTE-061 trial failed to demonstrate a significant survival improvement in PD-L1-positive GC patients [160].

Another phase 3 trial, CheckMate-649, demonstrated the efficacy of nivolumab in combination with fluoropyrimidine and platinum-based chemotherapy as a first-line treatment for HER2-negative advanced or metastatic GC, gastroesophageal junction cancer, and esophageal adenocarcinoma patients with PD-L1 CPS ≥ 5 [161]. In that trial, PD-L1 expression was determined using the PD-L1 IHC 28-8 pharmDx assay on the Autostainer Link 48 platform. Recently, that assay earned the CE-IVD mark in Europe as a companion diagnostic for identifying candidates for nivolumab treatment.

Both assays share the CPS scoring system to determine PD-L1 expression, which is the number of PD-L1–stained cells (tumor cells, lymphocytes, and macrophages) divided by the total number of viable tumor cells, multiplied by 100. For adequate evalu-

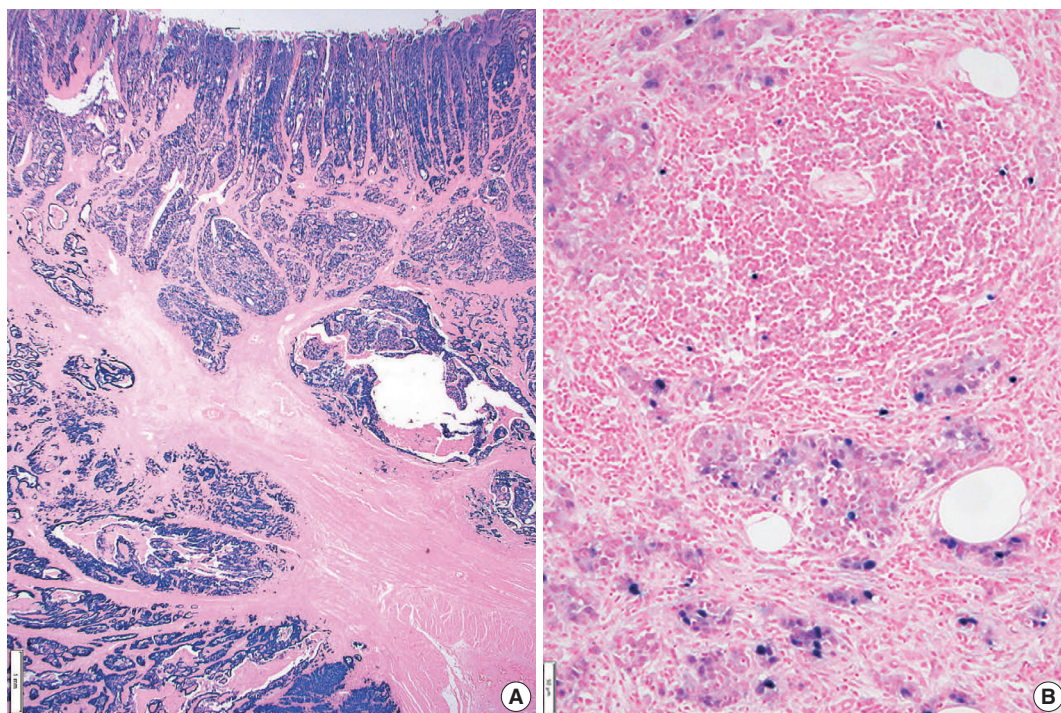


Fig. 13. A representative figure of Epstein-Barr virus (EBV) in situ hybridization. Diffuse positive EBV-encoded small RNA (EBER) signals (A). Heterogenous pattern of EBER signals in cancer cells. EBER signals appear within a few intratumoral lymphocytes (B).

ation, a specimen containing a minimum of 100 viable tumor cells is required [162]. A PD-L1–stained tumor cell should present partial or complete membrane staining of viable cells with more than faint staining intensity ($\geq 1+$). PD-L1–stained immune cells include only mononuclear inflammatory cells (lymphocytes or macrophages) within tumor nests and adjacent stroma and show membrane and/or cytoplasmic staining. Other stromal cells such as fibroblasts, neutrophils, and plasma cells should be excluded from the CPS numerator. If the result of the calculation exceeds 100, it is presented as a maximum score of 100. If the PD-L1 staining shows heterogeneous results, the final CPS should be estimated by calculating each area's CPS result (Fig. 14).

Because two different PD-L1 assays have been approved based on different CPS cutoff values, the interpretation of PD-L1 positivity should be based on the CPS cutoff value appropriate to the assay used for evaluation. The PD-L1 IHC 22C3 pharmDx assay uses CPS ≥ 1 for CPS positivity, and the 28-8 pharmDx assay uses CPS ≥ 5 . The report should specify the assay type and appropriate cutoff value used for the PD-L1 positivity interpretation.

Previous studies have reported changes in PD-L1 expression during chemotherapy [163,164] and discrepancies between primary and metastatic lesions [164,165]. Therefore, re-evaluation of PD-L1 IHC in secondary, recurrent, and metastatic lesions is recommended for GC patients.

Next generation sequencing

Recently identified molecular profiles are not only important for improving our understanding of driver alterations involved in gastric carcinogenesis, but also for identifying clinically relevant biomarkers and new potential therapeutic targets [124,125]. Therefore, the clinical need for NGS in AGCs is increasing.

According to the recent National Comprehensive Cancer Network (NCCN) guideline, the biomarkers implicated in clinical management of AGC include HER2, MSI, PD-L1, tumor mutation burden (TMB) status, and neurotrophic tyrosine receptor kinase (*NTRK*) gene fusion [100]. Among these, TMB can only be assessed using NGS, and *NTRK* fusion is best evaluated using NGS (preferential RNA sequencing) [166]. Alternatively, it can be screened with TRK IHC, and then sequencing can be performed in positive cases [166]. Some other targets also showed promising clinical results in advanced GC, such as fibroblast growth factor receptor 2 (*FGFR2*) amplification [167], epidermal growth factor receptor (*EGFR*) amplification [168], *MET* amplification [169], and alterations of homologous recombination deficiency–related genes [170]. In addition, there are very rare (prevalence $<1\%$) targetable tissue–agnostic variants [171] such as *BRAF* V600E [172], anaplastic lymphoma kinase (*ALK*) fusion [173], and reactive oxygen species 1 (*ROS1*) fusion [174].

TMB is defined as the total number of somatic coding muta-

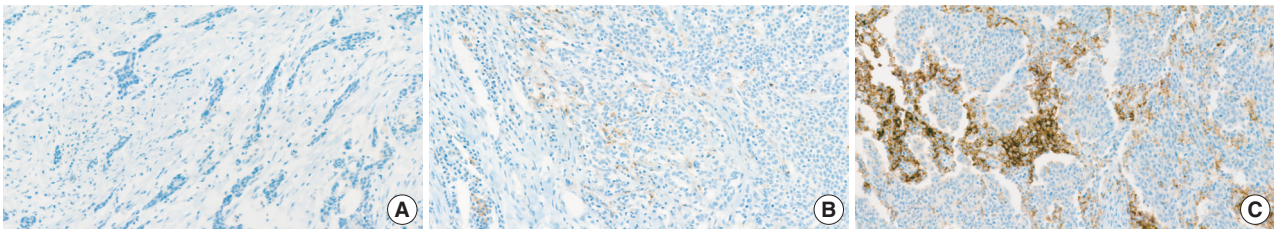


Fig. 14. A representative example of programmed death ligand 1 staining. Combined positive score (CPS) < 1 (A), CPS > 1 and < 5 (B), CPS > 5 (C).

tions in a tumor and represents an emerging biomarker for immunotherapy response in cancer patients [175]. The exploratory analysis for KEYNOTE-062 suggested an association between TMB and the clinical efficacy of first-line pembrolizumab-based therapy in patients with advanced GC [176]. Although whole exome sequencing is considered the gold standard for TMB, recent targeted gene panels have also provided accurate quantification [175]. The lack of harmonization in panel-based TMB quantification and lack of robust predictive cutoffs are currently some of the main limitations of TMB as a biomarker in clinical practice [175].

The gold standard for MSI detection is PCR or IHC. Recently, several MSI detection methods based on NGS have shown high concordance (> 95%) with the conventional PCR-based assay [171,177,178]. The recent NCCN guidelines indicate that sequencing via a validated NGS assay may be used to determine MSI status and other biomarkers when limited tissue is available for testing [100].

Tissue preparation is one of the most important factors for getting accurate and reliable results from NGS. In general, the total DNA and RNA requirements range from 10 to 300 ng for targeted gene panels [179]. Tissue specimen requirements are formalin-fixed, paraffin-embedded tissue or cytology specimens [179]. The minimum sample requirement for reliable sequencing results is a specimen with a tumor fraction and surface area > 10%–20% and 5 mm², respectively [179].

Mucin phenotype

GC is classified as the gastric type, intestinal type, mixed type, or unclassified type based on the expression of MUC5AC, MUC6, MUC2, and CD10 [3]. The gastric type is positive for MUC5AC and/or MUC6, and the intestinal type is positive for MUC2 and/or CD10. The mixed type is positive for both gastric and intestinal mucins, and the unclassified type is negative for both.

Easy methods for molecular classification

Molecular profiles of GCs have been published in recent stud-

ies by TCGA and the Asian Cancer Research Group (ACRG). TCGA classified GCs into EBV, MSI, genomically stable, and chromosomally unstable [124]. In contrast, ACRG published a molecular classification of MSI, microsatellite stable/epithelial mesenchymal transition (MSS/EMT), MSS/TP53+, and MSS/TP53– [125]. The MSS/EMT subtype is closely associated with the SRC and PCC histology and Lauren's diffuse type, and patient survival is poor. The EBV and MSI subtypes are related to the histologic type of adenocarcinoma with lymphoid stroma and have relatively better prognosis. High TMB and increased expression of PD-L1 are commonly reported in the EBV and MSI subtypes.

Several studies have reported that these molecular classifications could be reproduced in GCs using simple techniques, including EBV ISH, MSI testing, MMR IHC, E-cadherin IHC, and p53 IHC [127,180,181]. Using those tests, GC is classified as EBV, MSI, EMT, altered p53, and not altered p53. Those molecular subtypes showed distinct clinicopathologic characteristics.

Supplementary Information

The Data Supplement is available with this article at <https://doi.org/10.4132/jptm.2022.12.23>.

Ethics Statement

Not applicable.

Availability of Data and Material

Data sharing not applicable to this article as no datasets were generated or analyzed during the study.

Code Availability

Not applicable.

ORCID

Young Soo Park	https://orcid.org/0000-0001-5389-4245
Myeong-Cherl Kook	https://orcid.org/0000-0002-3435-3301
Baek-hui Kim	https://orcid.org/0000-0001-6793-1991
Hye Seung Lee	https://orcid.org/0000-0002-1667-7986
Dong-Wook Kang	https://orcid.org/0000-0002-4300-3469
Mi-Jin Gu	https://orcid.org/0000-0002-8350-3038
Ok Ran Shin	https://orcid.org/0000-0003-4506-5150
Younghee Choi	https://orcid.org/0000-0002-3882-4000

Wonaee Lee <https://orcid.org/0000-0001-9266-6640>
 Hyunki Kim <https://orcid.org/0000-0003-2292-5584>
 In Hye Song <https://orcid.org/0000-0001-6325-3548>
 Kyoung-Mee Kim <https://orcid.org/0000-0002-1162-9205>
 Hee Sung Kim <https://orcid.org/0000-0002-8154-2391>
 Guhyun Kang <https://orcid.org/0000-0001-7730-1686>
 Do Youn Park <https://orcid.org/0000-0001-7641-1509>
 So-Young Jin <https://orcid.org/0000-0002-9900-8322>
 Joon Mee Kim <https://orcid.org/0000-0003-1355-4187>
 Yoon Jung Choi <https://orcid.org/0000-0002-5701-8864>
 Hee Kyung Chang <https://orcid.org/0000-0002-4843-5316>
 Soomin Ahn <https://orcid.org/0000-0002-1979-4010>
 Mee Soo Chang <https://orcid.org/0000-0002-0948-799X>
 Song-Hee Han <https://orcid.org/0000-0002-4564-7014>
 Yoonjin Kwak <https://orcid.org/0000-0001-5314-2465>
 An Na Seo <https://orcid.org/0000-0001-6412-3067>
 Sung Hak Lee <https://orcid.org/0000-0003-1020-5838>
 Mee-Yon Cho <https://orcid.org/0000-0002-7955-4211>

Author Contributions

Conceptualization: YSP, MCK, BHK, HSL, KMK, JMK, SHL, MYC. Project administration: KMK, JMK, SHL, MYC. Supervision: DWK, YC, HK, KMK, DYP, SYJ, JMK, YJC, HKC, MSC, MYC. Writing—original draft preparation: YSP, MCK, BHK, HSL, SHL. Writing—review & editing: YSP, MCK, BHK, HSL, DWK, MJG, ORS, YC, WL, HK, HIS, KMK, HSK, GK, DYP, SYJ, JMK, YJC, HKC, SA, MSC, SHH, YK, ANS, SHL, MYC. Approval of final manuscript: all authors.

Conflicts of Interest

S.H.L., a contributing editor of the *Journal of Pathology and Translational Medicine*, was not involved in the editorial evaluation or decision to publish this article. All remaining authors have declared no conflicts of interest.

Funding Statement

This research was supported by a grant of Patient-Centered Clinical Research Coordinating Center (PACEN) funded by the Ministry of Health & Welfare, Republic of Korea (grant number: HC20C0123).

References

1. Sung H, Ferlay J, Siegel RL, et al. Global cancer statistics 2020: GLOBOCAN estimates of incidence and mortality worldwide for 36 cancers in 185 countries. *CA Cancer J Clin* 2021; 71: 209-49.
2. Hong S, Won YJ, Lee JJ, et al. Cancer statistics in Korea: incidence, mortality, survival, and prevalence in 2018. *Cancer Res Treat* 2021; 53: 301-15.
3. Kim WH, Park CK, Kim YB, et al. A standardized pathology report for gastric cancer. *Korean J Pathol* 2005; 39: 106-13.
4. World Health Organization. WHO classification of tumours: digestive system tumours. Geneva: World Health Organization, 2019.
5. Guideline Committee of the Korean Gastric Cancer Association (KGCA), Development Working Group and Review Panel. Korean practice guideline for gastric cancer 2018: an evidence-based, multi-disciplinary approach. *J Gastric Cancer* 2019; 19: 1-48.
6. Muro K, Chung HC, Shankaran V, et al. Pembrolizumab for patients with PD-L1-positive advanced gastric cancer (KEYNOTE-012): a multicentre, open-label, phase 1b trial. *Lancet Oncol* 2016; 17: 717-26.
7. Bang YJ, Van Cutsem E, Feyereislova A, et al. Trastuzumab in combination with chemotherapy versus chemotherapy alone for treat-

- ment of HER2-positive advanced gastric or gastro-oesophageal junction cancer (ToGA): a phase 3, open-label, randomised controlled trial. *Lancet* 2010; 376: 687-97.
8. Amin MB, Edge SB, Greene FL, et al. *AJCC cancer staging manual*. 8th ed. Cham: Springer, 2017.
9. Japanese Gastric Cancer Association. Japanese classification of gastric carcinoma: 3rd English edition. *Gastric Cancer* 2011; 14: 101-12.
10. Fritz A, Percy C, Jack A, et al. *International Classification of Diseases for Oncology (ICD-O)*. 3rd ed. Lyon: International Agency for Research on Cancer, 2013.
11. Shi C, Berlin J, Branton PA, et al. Protocol for the examination of specimens from patients with carcinoma of the stomach [Internet]. Northfield: College of American Pathologists, 2020 [cited 2022 Dec 1]. Available from: <https://documents.cap.org/protocols/cp-gi-upper-esophagus-20-4100.pdf>.
12. Shi C, Badgwell BD, Grabsch HI, et al. Data set for reporting carcinoma of the stomach in gastrectomy. *Arch Pathol Lab Med* 2022; 146: 1072-83.
13. Cunningham D, Allum WH, Stenning SP, et al. Perioperative chemotherapy versus surgery alone for resectable gastroesophageal cancer. *N Engl J Med* 2006; 355: 11-20.
14. Zhang X, Liang H, Li Z, et al. Perioperative or postoperative adjuvant oxaliplatin with S-1 versus adjuvant oxaliplatin with capecitabine in patients with locally advanced gastric or gastro-oesophageal junction adenocarcinoma undergoing D2 gastrectomy (RESOLVE): an open-label, superiority and non-inferiority, phase 3 randomised controlled trial. *Lancet Oncol* 2021; 22: 1081-92.
15. Kang YK, Yook JH, Park YK, et al. PRODIGY: a phase III study of neoadjuvant docetaxel, oxaliplatin, and S-1 plus surgery and adjuvant S-1 versus surgery and adjuvant S-1 for resectable advanced gastric cancer. *J Clin Oncol* 2021; 39: 2903-13.
16. Langer R, Becker K. Tumor regression grading of gastrointestinal cancers after neoadjuvant therapy. *Virchows Arch* 2018; 472: 175-86.
17. Mandard AM, Dalibard F, Mandard JC, et al. Pathologic assessment of tumor regression after preoperative chemoradiotherapy of esophageal carcinoma: clinicopathologic correlations. *Cancer* 1994; 73: 2680-6.
18. Dworak O, Keilholz L, Hoffmann A. Pathological features of rectal cancer after preoperative radiochemotherapy. *Int J Colorectal Dis* 1997; 12: 19-23.
19. Becker K, Mueller JD, Schulmacher C, et al. Histomorphology and grading of regression in gastric carcinoma treated with neoadjuvant chemotherapy. *Cancer* 2003; 98: 1521-30.
20. Mirza A, Naveed A, Hayes S, et al. Assessment of histopathological response in gastric and gastro-oesophageal junction adenocarcinoma following neoadjuvant chemotherapy: which scoring system to use? *ISRN Pathol* 2012; 2012: 519351.
21. Karamitopoulou E, Thies S, Zlobec I, et al. Assessment of tumor regression of esophageal adenocarcinomas after neoadjuvant chemotherapy: comparison of 2 commonly used scoring approaches. *Am J Surg Pathol* 2014; 38: 1551-6.
22. Kim BH, Kim JM, Kang GH, et al. Standardized pathology report for colorectal cancer, 2nd edition. *J Pathol Transl Med* 2020; 54: 1-19.
23. Tsekrekos A, Vieth M, Ndegwa N, et al. Interobserver agreement of a gastric adenocarcinoma tumor regression grading system that

- incorporates assessment of lymph nodes. *Hum Pathol* 2021; 116: 94-101.
24. Davies AR, Myoteri D, Zylstra J, et al. Lymph node regression and survival following neoadjuvant chemotherapy in oesophageal adenocarcinoma. *Br J Surg* 2018; 105: 1639-49.
 25. Reim D, Novotny A, Friess H, et al. Significance of tumour regression in lymph node metastases of gastric and gastro-oesophageal junction adenocarcinomas. *J Pathol Clin Res* 2020; 6: 263-72.
 26. Smyth EC, Fassan M, Cunningham D, et al. Effect of pathologic tumor response and nodal status on survival in the Medical Research Council adjuvant gastric infusional chemotherapy Trial. *J Clin Oncol* 2016; 34: 2721-7.
 27. Koh YW, Park YS, Ryu MH, et al. Postoperative nodal status and diffuse-type histology are independent prognostic factors in resectable advanced gastric carcinomas after preoperative chemotherapy. *Am J Surg Pathol* 2013; 37: 1022-9.
 28. Veronese N, Fassan M, Wood LD, et al. Extranodal extension of nodal metastases is a poor prognostic indicator in gastric cancer: a systematic review and meta-analysis. *J Gastrointest Surg* 2016; 20: 1692-8.
 29. Lee IS, Park YS, Ryu MH, et al. Impact of extranodal extension on prognosis in lymph node-positive gastric cancer. *Br J Surg* 2014; 101: 1576-84.
 30. Lee IS, Kang HJ, Park YS, et al. Prognostic impact of extranodal extension in stage 1B gastric carcinomas. *Surg Oncol* 2018; 27: 299-305.
 31. Araki I, Hosoda K, Yamashita K, et al. Prognostic impact of venous invasion in stage 1B node-negative gastric cancer. *Gastric Cancer* 2015; 18: 297-305.
 32. Takeuchi A, Ojima T, Katsuda M, et al. Venous invasion is a risk factor for recurrence of pT1 gastric cancer with lymph node metastasis. *J Gastrointest Surg* 2022; 26: 757-63.
 33. Nishibeppu K, Komatsu S, Ichikawa D, et al. Venous invasion as a risk factor for recurrence after gastrectomy followed by chemotherapy for stage III gastric cancer. *BMC Cancer* 2018; 18: 108.
 34. Liebig C, Ayala G, Wilks JA, Berger DH, Albo D. Perineural invasion in cancer: a review of the literature. *Cancer* 2009; 115: 3379-91.
 35. Hanaoka N, Tanabe S, Mikami T, Okayasu I, Saigenji K. Mixed-histologic-type submucosal invasive gastric cancer as a risk factor for lymph node metastasis: feasibility of endoscopic submucosal dissection. *Endoscopy* 2009; 41: 427-32.
 36. Takizawa K, Ono H, Kakushima N, et al. Risk of lymph node metastases from intramucosal gastric cancer in relation to histological types: how to manage the mixed histological type for endoscopic submucosal dissection. *Gastric Cancer* 2013; 16: 531-6.
 37. Lee JH, Choi IJ, Han HS, et al. Risk of lymph node metastasis in differentiated type mucosal early gastric cancer mixed with minor undifferentiated type histology. *Ann Surg Oncol* 2015; 22: 1813-9.
 38. Sekiguchi M, Oda I, Taniguchi H, et al. Risk stratification and predictive risk-scoring model for lymph node metastasis in early gastric cancer. *J Gastroenterol* 2016; 51: 961-70.
 39. Seo HS, Lee GE, Kang MG, Han KH, Jung ES, Song KY. Mixed histology is a risk factor for lymph node metastasis in early gastric cancer. *J Surg Res* 2019; 236: 271-7.
 40. Horiuchi Y, Ida S, Yamamoto N, et al. Feasibility of further expansion of the indications for endoscopic submucosal dissection in undifferentiated-type early gastric cancer. *Gastric Cancer* 2020; 23: 285-92.
 41. Ha TK, An JY, Youn HK, Noh JH, Sohn TS, Kim S. Indication for endoscopic mucosal resection in early signet ring cell gastric cancer. *Ann Surg Oncol* 2008; 15: 508-13.
 42. Kim BS, Oh ST, Yook JH, Kim BS. Signet ring cell type and other histologic types: differing clinical course and prognosis in T1 gastric cancer. *Surgery* 2014; 155: 1030-5.
 43. Guo CG, Zhao DB, Liu Q, et al. Risk factors for lymph node metastasis in early gastric cancer with signet ring cell carcinoma. *J Gastrointest Surg* 2015; 19: 1958-65.
 44. Huh CW, Jung DH, Kim JH, et al. Signet ring cell mixed histology may show more aggressive behavior than other histologies in early gastric cancer. *J Surg Oncol* 2013; 107: 124-9.
 45. Lee IS, Lee S, Park YS, Gong CS, Yook JH, Kim BS. Applicability of endoscopic submucosal dissection for undifferentiated early gastric cancer: Mixed histology of poorly differentiated adenocarcinoma and signet ring cell carcinoma is a worse predictive factor of nodal metastasis. *Surg Oncol* 2017; 26: 8-12.
 46. Kim YH, Park JH, Park CK, et al. Histologic purity of signet ring cell carcinoma is a favorable risk factor for lymph node metastasis in poorly cohesive, submucosa-invasive early gastric carcinoma. *Gastric Cancer* 2017; 20: 583-90.
 47. Chu Y, Mao T, Li X, et al. Predictors of lymph node metastasis and differences between pure and mixed histologic types of early gastric signet-ring cell carcinomas. *Am J Surg Pathol* 2020; 44: 934-42.
 48. Japanese Gastric Cancer Society. Regulations for the treatment of gastric cancer. 15th ed. Tokyo: Kanehara Publishing, 2017.
 49. Kim JY, Kim WG, Jeon TY, et al. Lymph node metastasis in early gastric cancer: evaluation of a novel method for measuring submucosal invasion and development of a nodal predicting index. *Hum Pathol* 2013; 44: 2829-36.
 50. Ma DW, Lee SJ, Kook MC, et al. The suggestion of revised criteria for endoscopic resection of differentiated-type submucosal gastric cancer. *Ann Surg Oncol* 2020; 27: 795-801.
 51. Choi JY, Park YS, Jung HY, et al. Identifying predictors of lymph node metastasis after endoscopic resection in patients with minute submucosal cancer of the stomach. *Surg Endosc* 2015; 29: 1476-83.
 52. Gotoda T, Yanagisawa A, Sasako M, et al. Incidence of lymph node metastasis from early gastric cancer: estimation with a large number of cases at two large centers. *Gastric Cancer* 2000; 3: 219-25.
 53. Park SM, Kim BW, Kim JS, Kim YW, Kim GJ, Ryu SJ. Can endoscopic ulcerations in early gastric cancer be clearly defined before endoscopic resection? A survey among endoscopists. *Clin Endosc* 2017; 50: 473-8.
 54. Kim JM, Sohn JH, Cho MY, et al. Pre- and post-ESD discrepancies in clinicopathologic criteria in early gastric cancer: the NECA-Korea ESD for Early Gastric Cancer Prospective Study (N-Keep). *Gastric Cancer* 2016; 19: 1104-13.
 55. Yabuuchi Y, Takizawa K, Kakushima N, et al. Discrepancy between endoscopic and pathological ulcerative findings in clinical intramucosal early gastric cancer. *Gastric Cancer* 2021; 24: 691-700.
 56. Shimoda T, Kushima R, Ono H. Histological features of peptic ulceration and biopsy scar of gastric ESD specimen. *Stomach Intestine* 2013; 48: 16-24.

57. Japanese Gastric Cancer Association. Japanese gastric cancer treatment guidelines 2018 (5th edition). *Gastric Cancer* 2021; 24: 1-21.
58. Takizawa K, Ono H, Hasuike N, et al. A nonrandomized, single-arm confirmatory trial of expanded endoscopic submucosal dissection indication for undifferentiated early gastric cancer: Japan Clinical Oncology Group study (JCOG1009/1010). *Gastric Cancer* 2021; 24: 479-91.
59. Hatta W, Gotoda T, Oyama T, et al. A scoring system to stratify curability after endoscopic submucosal dissection for early gastric cancer: "eCura system". *Am J Gastroenterol* 2017; 112: 874-81.
60. Uesugi N, Sugai T, Sugimoto R, et al. Clinicopathological and molecular stability and methylation analyses of gastric papillary adenocarcinoma. *Pathology* 2017; 49: 596-603.
61. Lee HJ, Kim GH, Park DY, et al. Endoscopic submucosal dissection for papillary adenocarcinoma of the stomach: is it really safe? *Gastric Cancer* 2017; 20: 978-86.
62. Min BH, Byeon SJ, Lee JH, et al. Lymphovascular invasion and lymph node metastasis rates in papillary adenocarcinoma of the stomach: implications for endoscopic resection. *Gastric Cancer* 2018; 21: 680-8.
63. Yasuda K, Adachi Y, Shiraishi N, Maeo S, Kitano S. Papillary adenocarcinoma of the stomach. *Gastric Cancer* 2000; 3: 33-8.
64. Yu H, Fang C, Chen L, et al. Worse prognosis in papillary, compared to tubular, early gastric carcinoma. *J Cancer* 2017; 8: 117-23.
65. Kawamura H, Kondo Y, Osawa S, et al. A clinicopathologic study of mucinous adenocarcinoma of the stomach. *Gastric Cancer* 2001; 4: 83-6.
66. Lee HH, Song KY, Park CH, Jeon HM. Undifferentiated-type gastric adenocarcinoma: prognostic impact of three histological types. *World J Surg Oncol* 2012; 10: 254.
67. Nakamura K, Eto K, Iwagami S, et al. Clinicopathological characteristics and prognosis of poorly cohesive cell subtype of gastric cancer. *Int J Clin Oncol* 2022; 27: 512-9.
68. Roviello F, Marano L, Ambrosio MR, et al. Signet ring cell percentage in poorly cohesive gastric cancer patients: a potential novel predictor of survival. *Eur J Surg Oncol* 2022; 48: 561-9.
69. Garcia-Pelaez J, Barbosa-Matos R, Gullo I, Carneiro F, Oliveira C. Histological and mutational profile of diffuse gastric cancer: current knowledge and future challenges. *Mol Oncol* 2021; 15: 2841-67.
70. Kwon CH, Kim YK, Lee S, et al. Gastric poorly cohesive carcinoma: a correlative study of mutational signatures and prognostic significance based on histopathological subtypes. *Histopathology* 2018; 72: 556-68.
71. Mariette C, Carneiro F, Grabsch HI, et al. Consensus on the pathological definition and classification of poorly cohesive gastric carcinoma. *Gastric Cancer* 2019; 22: 1-9.
72. Han JP, Hong SJ, Kim HK. Long-term outcomes of early gastric cancer diagnosed as mixed adenocarcinoma after endoscopic submucosal dissection. *J Gastroenterol Hepatol* 2015; 30: 316-20.
73. Park HK, Lee KY, Yoo MW, Hwang TS, Han HS. Mixed carcinoma as an independent prognostic factor in submucosal invasive gastric carcinoma. *J Korean Med Sci* 2016; 31: 866-72.
74. Horiuchi Y, Fujisaki J, Yamamoto N, et al. Undifferentiated-type predominant mixed-type early gastric cancer is a significant risk factor for requiring additional surgeries after endoscopic submucosal dissection. *Sci Rep* 2020; 10: 6748.
75. Ozeki Y, Hirasawa K, Sawada A, et al. Mixed histology poses a greater risk for noncurative endoscopic resection in early gastric cancers regardless of the predominant histologic types. *Eur J Gastroenterol Hepatol* 2021; 32: 186-93.
76. Shin DH, Kim GH, Lee BE, et al. Clinicopathologic features of early gastric carcinoma with lymphoid stroma and feasibility of endoscopic submucosal dissection. *Surg Endosc* 2017; 31: 4156-64.
77. Iwasaki K, Suda T, Takano Y, et al. Postoperative outcomes of gastric carcinoma with lymphoid stroma. *World J Surg Oncol* 2020; 18: 102.
78. Huh CW, Jung DH, Kim H, et al. Clinicopathologic features of gastric carcinoma with lymphoid stroma in early gastric cancer. *J Surg Oncol* 2016; 114: 769-72.
79. Inagawa S, Shimazaki J, Hori M, et al. Hepatoid adenocarcinoma of the stomach. *Gastric Cancer* 2001; 4: 43-52.
80. Roh JH, Srivastava A, Lauwers GY, et al. Micropapillary carcinoma of stomach: a clinicopathologic and immunohistochemical study of 11 cases. *Am J Surg Pathol* 2010; 34: 1139-46.
81. Fujita T, Gotohda N, Kato Y, et al. Clinicopathological features of stomach cancer with invasive micropapillary component. *Gastric Cancer* 2012; 15: 179-87.
82. Benedict MA, Lauwers GY, Jain D. Gastric adenocarcinoma of the fundic gland type: update and literature review. *Am J Clin Pathol* 2018; 149: 461-73.
83. Miyazawa M, Matsuda M, Yano M, et al. Gastric adenocarcinoma of the fundic gland (chief cell-predominant type): a review of endoscopic and clinicopathological features. *World J Gastroenterol* 2016; 22: 10523-31.
84. Agaimy A, Rau TT, Hartmann A, Stoehr R. SMARCB1 (INI1)-negative rhabdoid carcinomas of the gastrointestinal tract: clinicopathologic and molecular study of a highly aggressive variant with literature review. *Am J Surg Pathol* 2014; 38: 910-20.
85. Willems S, Carneiro F, Geboes K. Gastric carcinoma with osteoclast-like giant cells and lymphoepithelioma-like carcinoma of the stomach: two of a kind? *Histopathology* 2005; 47: 331-3.
86. Woo HY, Bae YS, Kim JH, et al. Distinct expression profile of key molecules in crawling-type early gastric carcinoma. *Gastric Cancer* 2017; 20: 612-9.
87. Okamoto N, Kawachi H, Yoshida T, et al. "Crawling-type" adenocarcinoma of the stomach: a distinct entity preceding poorly differentiated adenocarcinoma. *Gastric Cancer* 2013; 16: 220-32.
88. Ushiku T, Kunita A, Kuroda R, et al. Oxyntic gland neoplasm of the stomach: expanding the spectrum and proposal of terminology. *Mod Pathol* 2020; 33: 206-16.
89. Tsuji Y, Ushiku T, Shinozaki T, et al. Risk for lymph node metastasis in Epstein-Barr virus-associated gastric carcinoma with submucosal invasion. *Dig Endosc* 2021; 33: 592-7.
90. Lauren P. The two histological main types of gastric carcinoma: diffuse and so-called intestinal-type carcinoma: an attempt at a histo-clinical classification. *Acta Pathol Microbiol Scand* 1965; 64: 31-49.
91. Park DY, Srivastava A, Kim GH, et al. Adenomatous and foveolar gastric dysplasia: distinct patterns of mucin expression and background intestinal metaplasia. *Am J Surg Pathol* 2008; 32: 524-33.
92. Choi WT, Brown I, Ushiku T, et al. Gastric pyloric gland adenoma: a multicentre clinicopathological study of 67 cases. *Histopa-*

- thology 2018; 72: 1007-14.
93. Kim JM, Sohn JH, Cho MY, et al. Inter-observer reproducibility in the pathologic diagnosis of gastric intraepithelial neoplasia and early carcinoma in endoscopic submucosal dissection specimens: a multi-center study. *Cancer Res Treat* 2019; 51: 1568-77.
 94. Kim JM, Cho MY, Sohn JH, et al. Diagnosis of gastric epithelial neoplasia: dilemma for Korean pathologists. *World J Gastroenterol* 2011; 17: 2602-10.
 95. Watanabe Y, Shimizu M, Itoh T, Nagashima K. Intraglandular necrotic debris in gastric biopsy and surgical specimens. *Ann Diagn Pathol* 2001; 5: 141-7.
 96. Choi IJ, Kook MC, Kim YI, et al. *Helicobacter pylori* therapy for the prevention of metachronous gastric cancer. *N Engl J Med* 2018; 378: 1085-95.
 97. Ono H, Yao K, Fujishiro M, et al. Guidelines for endoscopic submucosal dissection and endoscopic mucosal resection for early gastric cancer (second edition). *Dig Endosc* 2021; 33: 4-20.
 98. Shitara K, Bang YJ, Iwasa S, et al. Trastuzumab deruxtecan in previously treated HER2-positive gastric cancer. *N Engl J Med* 2020; 382: 2419-30.
 99. FDA approves fam-trastuzumab deruxtecan-nxki for HER2-positive gastric adenocarcinomas [Internet]. Silver Spring: U.S. Food and Drug Administration, 2021 [cited 2022 Dec 1]. Available from: <https://www.fda.gov/drugs/resources-information-approved-drugs/fda-approves-fam-trastuzumab-deruxtecan-nxki-her2-positive-gastric-adenocarcinomas>.
 100. Ajani JA, D'Amico TA, Bentrem DJ, et al. Gastric cancer, version 2.2022, NCCN Clinical Practice Guidelines in Oncology. *J Natl Compr Canc Netw* 2022; 20: 167-92.
 101. Hofmann M, Stoss O, Shi D, et al. Assessment of a HER2 scoring system for gastric cancer: results from a validation study. *Histopathology* 2008; 52: 797-805.
 102. Ahn S, Ahn S, Van Vrancken M, et al. Ideal number of biopsy tumor fragments for predicting HER2 status in gastric carcinoma resection specimens. *Oncotarget* 2015; 6: 38372-80.
 103. Lee HS, Kim WH, Kwak Y, et al. Molecular testing for gastrointestinal cancer. *J Pathol Transl Med* 2017; 51: 103-21.
 104. Bartley AN, Washington MK, Colasacco C, et al. HER2 testing and clinical decision making in gastroesophageal adenocarcinoma: guideline from the College of American Pathologists, American Society for Clinical Pathology, and the American Society of Clinical Oncology. *J Clin Oncol* 2017; 35: 446-64.
 105. Wolff AC, Hammond ME, Hicks DG, et al. Recommendations for human epidermal growth factor receptor 2 testing in breast cancer: American Society of Clinical Oncology/College of American Pathologists clinical practice guideline update. *J Clin Oncol* 2013; 31: 3997-4013.
 106. Van Cutsem E, Bang YJ, Feng-Yi F, et al. HER2 screening data from ToGA: targeting HER2 in gastric and gastroesophageal junction cancer. *Gastric Cancer* 2015; 18: 476-84.
 107. Tsapralis D, Panayiotides I, Peros G, Liakakos T, Karamitopoulou E. Human epidermal growth factor receptor-2 gene amplification in gastric cancer using tissue microarray technology. *World J Gastroenterol* 2012; 18: 150-5.
 108. Liu W, Zhong S, Chen J, Yu Y. HER-2/neu overexpression is an independent prognostic factor for intestinal-type and early-stage gastric cancer patients. *Journal of clinical gastroenterology* 2012; 46: e31-7.
 109. Lee HE, Park KU, Yoo SB, et al. Clinical significance of intratumoral HER2 heterogeneity in gastric cancer. *European Journal of Cancer* 2013; 49: 1448-57.
 110. Kim MA, Lee HJ, Yang HK, Bang YJ, Kim WH. Heterogeneous amplification of ERBB2 in primary lesions is responsible for the discordant ERBB2 status of primary and metastatic lesions in gastric carcinoma. *Histopathology* 2011; 59: 822-31.
 111. Peng Z, Zou J, Zhang X, et al. HER2 discordance between paired primary gastric cancer and metastasis: a meta-analysis. *Chin J Cancer Res* 2015; 27: 163-71.
 112. Kim JH, Kim MA, Lee HS, Kim WH. Comparative analysis of protein expressions in primary and metastatic gastric carcinomas. *Hum Pathol* 2009; 40: 314-22.
 113. Fusco N, Rocco EG, Del Conte C, et al. HER2 in gastric cancer: a digital image analysis in pre-neoplastic, primary and metastatic lesions. *Mod Pathol* 2013; 26: 816-24.
 114. Geng Y, Chen X, Qiu J, et al. Human epidermal growth factor receptor-2 expression in primary and metastatic gastric cancer. *Int J Clin Oncol* 2014; 19: 303-11.
 115. Kochi M, Fujii M, Masuda S, et al. Differing deregulation of HER2 in primary gastric cancer and synchronous related metastatic lymph nodes. *Diagn Pathol* 2013; 8: 191.
 116. Ieni A, Barresi V, Rigoli L, Caruso RA, Tuccari G. HER2 status in premalignant, early, and advanced neoplastic lesions of the stomach. *Dis Markers* 2015; 2015: 234851.
 117. Zhao W, Sun L, Dong G, Wang X, Jia Y, Tong Z. Receptor conversion impacts outcomes of different molecular subtypes of primary breast cancer. *Ther Adv Med Oncol* 2021; 13: 17588359211012982.
 118. Garrido-Ramos MA. Satellite DNA: an evolving topic. *Genes (Basel)* 2017; 8: 230.
 119. Luchini C, Bibeau F, Ligtenberg MJL, et al. ESMO recommendations on microsatellite instability testing for immunotherapy in cancer, and its relationship with PD-1/PD-L1 expression and tumour mutational burden: a systematic review-based approach. *Ann Oncol* 2019; 30: 1232-43.
 120. Li K, Luo H, Huang L, Luo H, Zhu X. Microsatellite instability: a review of what the oncologist should know. *Cancer Cell Int* 2020; 20: 16.
 121. Jiricny J. Postreplicative mismatch repair. *Cold Spring Harb Perspect Biol* 2013; 5: a012633.
 122. Ma J, Setton J, Lee NY, Riaz N, Powell SN. The therapeutic significance of mutational signatures from DNA repair deficiency in cancer. *Nat Commun* 2018; 9: 3292.
 123. Peltomaki P. Role of DNA mismatch repair defects in the pathogenesis of human cancer. *J Clin Oncol* 2003; 21: 1174-9.
 124. Cancer Genome Atlas Research Network. Comprehensive molecular characterization of gastric adenocarcinoma. *Nature* 2014; 513: 202-9.
 125. Cristescu R, Lee J, Nebozhyn M, et al. Molecular analysis of gastric cancer identifies subtypes associated with distinct clinical outcomes. *Nat Med* 2015; 21: 449-56.
 126. Setia N, Agoston AT, Han HS, et al. A protein and mRNA expression-based classification of gastric cancer. *Mod Pathol* 2016; 29: 772-84.
 127. Ahn S, Lee SJ, Kim Y, et al. High-throughput protein and mRNA expression-based classification of gastric cancers can identify clinically distinct subtypes, concordant with recent molecular classifications. *Am J Surg Pathol* 2017; 41: 106-15.

128. Choi YY, Kim H, Shin SJ, et al. Microsatellite instability and programmed cell death-ligand 1 expression in stage II/III gastric cancer: post hoc analysis of the CLASSIC randomized controlled study. *Ann Surg* 2019; 270: 309-16.
129. Guastadisegni C, Colafranceschi M, Ottini L, Dogliotti E. Microsatellite instability as a marker of prognosis and response to therapy: a meta-analysis of colorectal cancer survival data. *Eur J Cancer* 2010; 46: 2788-98.
130. Kim ST, Cristescu R, Bass AJ, et al. Comprehensive molecular characterization of clinical responses to PD-1 inhibition in metastatic gastric cancer. *Nat Med* 2018; 24: 1449-58.
131. Le DT, Uram JN, Wang H, et al. PD-1 blockade in tumors with mismatch-repair deficiency. *N Engl J Med* 2015; 372: 2509-20.
132. Le DT, Durham JN, Smith KN, et al. Mismatch repair deficiency predicts response of solid tumors to PD-1 blockade. *Science* 2017; 357: 409-13.
133. Ratti M, Lampis A, Hahne JC, Passalacqua R, Valeri N. Microsatellite instability in gastric cancer: molecular bases, clinical perspectives, and new treatment approaches. *Cell Mol Life Sci* 2018; 75: 4151-62.
134. Jang M, Kwon Y, Kim H, et al. Microsatellite instability test using peptide nucleic acid probe-mediated melting point analysis: a comparison study. *Bmc Cancer* 2018; 18: 1218.
135. Murphy KM, Zhang S, Geiger T, et al. Comparison of the microsatellite instability analysis system and the Bethesda panel for the determination of microsatellite instability in colorectal cancers. *J Mol Diagn* 2006; 8: 305-11.
136. Berg KD, Glaser CL, Thompson RE, Hamilton SR, Griffin CA, Esheleman JR. Detection of microsatellite instability by fluorescence multiplex polymerase chain reaction. *J Mol Diagn* 2000; 2: 20-8.
137. Deschoolmeester V, Baay M, Wuys W, et al. Detection of microsatellite instability in colorectal cancer using an alternative multiplex assay of quasi-monomorphic mononucleotide markers. *J Mol Diagn* 2008; 10: 154-9.
138. Shia J, Ellis NA, Klimstra DS. The utility of immunohistochemical detection of DNA mismatch repair gene proteins. *Virchows Arch* 2004; 445: 431-41.
139. McCarthy AJ, Capo-Chichi JM, Spence T, et al. Heterogenous loss of mismatch repair (MMR) protein expression: a challenge for immunohistochemical interpretation and microsatellite instability (MSI) evaluation. *J Pathol Clin Res* 2019; 5: 115-29.
140. Renkonen E, Zhang Y, Lohi H, et al. Altered expression of MLH1, MSH2, and MSH6 in predisposition to hereditary nonpolyposis colorectal cancer. *J Clin Oncol* 2003; 21: 3629-37.
141. Graham RP, Kerr SE, Butz ML, et al. Heterogenous MSH6 loss is a result of microsatellite instability within MSH6 and occurs in sporadic and hereditary colorectal and endometrial carcinomas. *Am J Surg Pathol* 2015; 39: 1370-6.
142. Jansson A, Arbman G, Zhang H, Sun XF. Combined deficiency of hMLH1, hMSH2, hMSH3 and hMSH6 is an independent prognostic factor in colorectal cancer. *Int J Oncol* 2003; 22: 41-9.
143. Ruzkiewicz A, Bennett G, Moore J, et al. Correlation of mismatch repair genes immunohistochemistry and microsatellite instability status in HNPCC-associated tumours. *Pathology* 2002; 34: 541-7.
144. Fukayama M, Abe H, Kunita A, et al. Thirty years of Epstein-Barr virus-associated gastric carcinoma. *Virchows Arch* 2020; 476: 353-65.
145. Chang MS, Kim DH, Roh JK, et al. Epstein-Barr virus-encoded BART1 promotes proliferation of gastric carcinoma cells through regulation of NF-kappaB. *J Virol* 2013; 87: 10515-23.
146. Hoebe EK, Le Large TY, Greijer AE, Middeldorp JM. BamHI-A rightward frame 1, an Epstein-Barr virus-encoded oncogene and immune modulator. *Rev Med Virol* 2013; 23: 367-83.
147. zur Hausen A, Brink AA, Craanen ME, Middeldorp JM, Meijer CJ, van den Brule AJ. Unique transcription pattern of Epstein-Barr virus (EBV) in EBV-carrying gastric adenocarcinomas: expression of the transforming BART1 gene. *Cancer Res* 2000; 60: 2745-8.
148. Kang GH, Lee S, Kim WH, et al. Epstein-barr virus-positive gastric carcinoma demonstrates frequent aberrant methylation of multiple genes and constitutes CpG island methylator phenotype-positive gastric carcinoma. *Am J Pathol* 2002; 160: 787-94.
149. Strong MJ, Xu G, Coco J, et al. Differences in gastric carcinoma microenvironment stratify according to EBV infection intensity: implications for possible immune adjuvant therapy. *PLoS Pathog* 2013; 9: e1003341.
150. Gu L, Chen M, Guo D, et al. PD-L1 and gastric cancer prognosis: a systematic review and meta-analysis. *PLoS One* 2017; 12: e0182692.
151. Park JH, Kim EK, Kim YH, et al. Epstein-Barr virus positivity, not mismatch repair-deficiency, is a favorable risk factor for lymph node metastasis in submucosa-invasive early gastric cancer. *Gastric Cancer* 2016; 19: 1041-51.
152. Cheng Y, Zhou X, Xu K, Huang J, Huang Q. Very low risk of lymph node metastasis in Epstein-Barr virus-associated early gastric carcinoma with lymphoid stroma. *BMC Gastroenterol* 2020; 20: 273.
153. Yoon CJ, Chang MS, Kim DH, et al. Epstein-Barr virus-encoded miR-BART5-5p upregulates PD-L1 through PIAS3/pSTAT3 modulation, worsening clinical outcomes of PD-L1-positive gastric carcinomas. *Gastric Cancer* 2020; 23: 780-95.
154. Lee HS, Chang MS, Yang HK, Lee BL, Kim WH. Epstein-barr virus-positive gastric carcinoma has a distinct protein expression profile in comparison with epstein-barr virus-negative carcinoma. *Clin Cancer Res* 2004; 10: 1698-705.
155. Longnecker RM, Kieff E, Cohen JI. Epstein-Barr virus. In: Knipe DM, Howley PM, eds. *Fields virology*. 6th ed. Philadelphia: Lippincott Williams & Wilkins, 2013; 1898-959.
156. Boger C, Kruger S, Behrens HM, et al. Epstein-Barr virus-associated gastric cancer reveals intratumoral heterogeneity of PIK3CA mutations. *Ann Oncol* 2017; 28: 1005-14.
157. Ribas A. Tumor immunotherapy directed at PD-1. *N Engl J Med* 2012; 366: 2517-9.
158. Kwak Y, Seo AN, Lee HE, Lee HS. Tumor immune response and immunotherapy in gastric cancer. *J Pathol Transl Med* 2020; 54: 20-33.
159. Fuchs CS, Doi T, Jang RW, et al. Safety and efficacy of pembrolizumab monotherapy in patients with previously treated advanced gastric and gastroesophageal junction cancer: phase 2 clinical KEYNOTE-059 trial. *JAMA Oncol* 2018; 4: e180013.
160. Shitara K, Ozguroglu M, Bang YJ, et al. Pembrolizumab versus paclitaxel for previously treated, advanced gastric or gastro-oesophageal junction cancer (KEYNOTE-061): a randomised, open-label, controlled, phase 3 trial. *Lancet* 2018; 392: 123-33.
161. Janjigian YY, Shitara K, Moehler M, et al. First-line nivolumab plus chemotherapy versus chemotherapy alone for advanced gastric, gastro-oesophageal junction, and oesophageal adenocarcinoma (CheckMate 649): a randomised, open-label, phase 3 trial. *Lan-*

- cet 2021; 398: 27-40.
162. DAKO Agilent Technologies. Interpretation manual: gastric or gastroesophageal junction adenocarcinoma. PD-L1 IHC 22C3 pharmDx interpretation manual: gastric or gastroesophageal junction adenocarcinoma. Santa Clara: DAKO Agilent Technologies, 2018.
 163. Yang JH, Kim H, Roh SY, et al. Discordancy and changes in the pattern of programmed death ligand 1 expression before and after platinum-based chemotherapy in metastatic gastric cancer. *Gastric Cancer* 2019; 22: 147-54.
 164. Zhou KI, Peterson B, Serritella A, et al. Spatial and temporal heterogeneity of PD-L1 expression and tumor mutational burden in gastroesophageal adenocarcinoma at baseline diagnosis and after chemotherapy. *Clin Cancer Res* 2020; 26: 6453-63.
 165. Son SM, Woo CG, Kim DH, et al. Distinct tumor immune microenvironments in primary and metastatic lesions in gastric cancer patients. *Sci Rep* 2020; 10: 14293.
 166. Marchio C, Scaltriti M, Ladanyi M, et al. ESMO recommendations on the standard methods to detect NTRK fusions in daily practice and clinical research. *Ann Oncol* 2019; 30: 1417-27.
 167. Catenacci DV, Rasco D, Lee J, et al. Phase I escalation and expansion study of bemarituzumab (FPA144) in patients with advanced solid tumors and FGFR2b-selected gastroesophageal adenocarcinoma. *J Clin Oncol* 2020; 38: 2418-26.
 168. Maron SB, Alpert L, Kwak HA, et al. Targeted therapies for targeted populations: anti-EGFR treatment for *EGFR*-amplified gastroesophageal adenocarcinoma. *Cancer Discov* 2018; 8: 696-713.
 169. Lee J, Kim ST, Kim K, et al. Tumor genomic profiling guides patients with metastatic gastric cancer to targeted treatment: the VIKTORY Umbrella Trial. *Cancer Discov* 2019; 9: 1388-405.
 170. Smyth EC, Cafferkey C, Loehr A, et al. Genomic loss of heterozygosity and survival in the REAL3 trial. *Oncotarget* 2018; 9: 36654-65.
 171. Nakamura Y, Kawazoe A, Lordick F, Janjigian YY, Shitara K. Biomarker-targeted therapies for advanced-stage gastric and gastroesophageal junction cancers: an emerging paradigm. *Nat Rev Clin Oncol* 2021; 18: 473-87.
 172. van Grieken NC, Aoyama T, Chambers PA, et al. *KRAS* and *BRAF* mutations are rare and related to DNA mismatch repair deficiency in gastric cancer from the East and the West: results from a large international multicentre study. *Br J Cancer* 2013; 108: 1495-501.
 173. Wen Z, Xiong D, Zhang S, et al. Case report: RAB10-ALK: a novel *ALK* fusion in a patient with gastric cancer. *Front Oncol* 2021; 11: 645370.
 174. Lee J, Lee SE, Kang SY, et al. Identification of *ROS1* rearrangement in gastric adenocarcinoma. *Cancer* 2013; 119: 1627-35.
 175. Fancello L, Gandini S, Pelicci PG, Mazzarella L. Tumor mutational burden quantification from targeted gene panels: major advancements and challenges. *J Immunother Cancer* 2019; 7: 183.
 176. Lee KW, Van Cutsem E, Bang YJ, et al. Association of tumor mutational burden with efficacy of pembrolizumab+/-chemotherapy as first-line therapy for gastric cancer in the phase III KEYNOTE-062 study. *Clin Cancer Res* 2022; 28: 3489-98.
 177. Kang SY, Kim DG, Ahn S, Ha SY, Jang KT, Kim KM. Comparative analysis of microsatellite instability by next-generation sequencing, MSI PCR and MMR immunohistochemistry in 1942 solid cancers. *Pathol Res Pract* 2022; 233: 153874.
 178. Ratovomanana T, Cohen R, Svrcek M, et al. Performance of next-generation sequencing for the detection of microsatellite instability in colorectal cancer with deficient DNA mismatch repair. *Gastroenterology* 2021; 161: 814-26.
 179. Ascierto PA, Bifulco C, Palmieri G, Peters S, Sidiropoulos N. Preanalytic variables and tissue stewardship for reliable next-generation sequencing (NGS) clinical analysis. *J Mol Diagn* 2019; 21: 756-67.
 180. Koh J, Lee KW, Nam SK, et al. Development and validation of an easy-to-implement, practical algorithm for the identification of molecular subtypes of gastric cancer: prognostic and therapeutic implications. *Oncologist* 2019; 24: e1321-30.
 181. Ramos M, Pereira MA, Amorim LC, et al. Gastric cancer molecular classification and adjuvant therapy: is there a different benefit according to the subtype? *J Surg Oncol* 2020; 121: 804-13.